F.F.
#65

50-247

WESTINGHOUSE NON-PROPRIETARY CLASS III

#500

PI-2 A

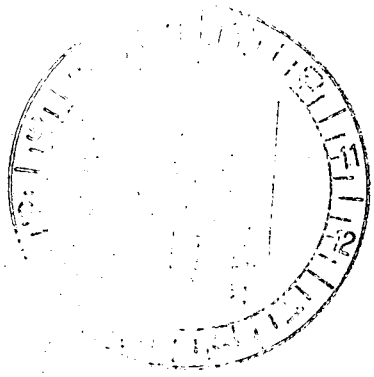

FUEL DENSIFICATION - INDIAN POINT NUCLEAR GENERATING STATION UNIT NO. 2

JANUARY, 1973

Material that is proprietary to the Westinghouse Electric Corporation has been deleted from this document.

TABLE OF CONTENTS

TABLE OF CONTENTS (Continued)

LIST OF TABLES

LIST OF FIGURES

LIST OF FIGURES (Continued)

1.0 INTRODUCTION AND SUMMARY

During the latter stages of construction of the Indian Point Unit No. 2 nuclear plant, the phenomenon of in-pile densification of UO_2 fuel was identified as a matter of concern in light water reactors. This report contains an evaluation of fuel densification as it relates to Indian Point Unit No. 2, and establishes that full rated power operation can be achieved, and presents proposed changes to the Technical Specifications consistent with that evaluation.

Densification of UO_2 fuel has been observed to occur under irradiation in several operating reactors. This densification causes pellets to shrink both axially and radially. The pellet shrinkage combined with random hang-up of fuel pellets results in gaps in the fuel column when the pellets below the hung-up pellet settle in the fuel rod. These gaps vary in length and location in the fuel rod. Because of increased moderation and decreased neutron absorptions in the vicinity of the gap, power peaking occurs in the adjacent fuel rods. The initial radial shrinkage of the pellet increases the clad-pellet radial gap and results in higher fuel temperatures. As months of operation are accumulated however, the clad creeps inward and fuel temperature decreases.

The major significance of these factors, generally, are the following:

a) The axial shrinkage of the pellet combined with power peaking due to gaps increases the power peaking factor. In Addition, the initially larger radial pellet-clad gap produces a higher fuel centerline temperature for a constant average linear power density. Thus, the limiting linear power density must be compatible with operation at full rated power or power penalty restrictions must be imposed.

b) The increased local power density and higher average fuel temperature must be taken into account in the analysis of the loss-of-coolant

accident to determine whether the fuel cladding temperature associated with full rated power operation can be maintained below 2300°F in the event of a LOCA.

To eliminate such penalties associated with fuel densification in Indian Point 2, it was decided to modify the design of the fuel. Thus, the original unpressurized fuel was returned from the reactor site to the factory to perform the modifications. Basically, these modifications consisted of (1) prepressurization of the fuel rods, (2) replacing the fuel pellets in Regions 2 and 3 with those of higher density (95% theoretical) and U-235 enrichment, and (3) increasing the number of burnable poison rods. Other changes in the core design are described in Section 3.

The determination of reactor power capability with the modified fuel was made following the methods described in WCAP-7984[1], "Fuel Densification Penalty Model," as modified according to the AEC fuel gap size[2] distribution. The conclusions presented in Section 5 are based on the premise that the fuel cladding in the regions of the fuel column gaps will not flatten during operation as justified in Section 2. The evaluation considered the fuel performance limits described in Section 4.

In Section 6, all of the accidents analyzed and reported in the FSAR[3] which could potentially be affected by fuel densification have been reviewed. The results for those requiring reanalysis and the justification of the applicability of previous results for the remainder are presented.

The Technical Specifications requiring change for the operations described have been reviewed and modified Technical Specifications have been proposed in Section 7.

It has been concluded that the operations of Indian Point Unit No. 2 with the modified core described herein can be carried out in conformity with the rules and regulations of the Atomic Energy Commission in a manner that provides reasonable assurance that such operation will not endanger the health and safety of the public.

References for Section 1

1. Eng, G., et al., "Fuel Densification Penalty Model," WCAP-7984, October, 1972.

2. "Technical Report on Densification of Light Water Reactor Fuels," Regulatory Staff U. S. A. E. C., November 14, 1972.

3. "Final Facility Description and Safety Analysis Report - Indian Point Nuclear Generating Station Unit No. 2," Docket No. 50-247.

2.0 CLAD FLATTENING ANALYSIS

Using current Westinghouse analytical techniques[1] and operating conditions appropriate for the "worst-case" lead burnup rods in each region of Indian Point 2, the following minimum time to clad flattening is predicted.

	Minimum time to clad flattening
Region 1	Greater than 21,000 EFPH* (nominal burnup for two cycles)
Region 2	Greater than 29,000 EFPH* (nominal burnup for three cycles)
Region 3	Greater than three cycles

*EFPH = Effective Full Power Hours, integrated flux equivalent to operating at 100% power at stated time.

No clad flattening is predicted in Indian Point 2 since the best estimates for cycles 2 and 3 burnups are less than the conservative, minimum calculated time for initial clad flattening.

Recent data from Point Beach No. 1 indicate that the analysis is conservative. Whereas the analysis predicted clad flattening in Regions 2 and 3 after [ ] EFPH, clad flattening was not observed after 13,000 EFPH, the end of the first cycle.

References for Section 2

1. Eng, G., et al., "Fuel Densification Penalty Model," WCAP-7984, October, 1972.

3.0 REACTOR

3.1 REACTOR DESIGN

A description of the Indian Point Unit No. 2 reactor core can be found in the FSAR.[1] The reactor core is a three-region cycled core with a rated power of 2758 MW thermal. It contains 193 fuel assemblies each containing 204 fuel rods. The fuel rods have a nominal active length of 12 ft. and contain enriched UO_2. The fuel rod cladding is Zircaloy-4, with a nominal O.D. of 0.422 in. and 0.0243 in. wall thickness. The UO_2 pellet is approximately 0.365 in. O.D. by 0.6 in. high with dished ends.

Due to fuel rod Zircaloy growth and fuel densification considerations, the fuel rods, fuel assembly and core loading pattern have been modified for the replacement core, as described in the following sections.

3.1.1 MECHANICAL DESIGN AND EVALUATION

This section supplements and modifies the corresponding Section 3.2.3 in the Indian Point Unit No. 2 FSAR.[1] The original Regions 2 and 3 unpressurized fuel rods have been replaced by new fuel rods which are prepressurized with helium to [ ] and which contain higher initial density (95% T.D.) fuel pellets. This change was made to minimize the potential effects due to fuel densification. The average fuel enrichments of Regions 2 and 3 have been increased by 0.1% to 2.8 and 3.3 w/o respectively. The increased fuel density and enrichment in the replacement core requires an increase in the number of burnable poison rods from 1160 to 1412 in order to avoid a positive moderator coefficient at BOL. The location of the fuel assemblies and the burnable poison rods in the core are described in the Nuclear Design Section. The Region 1 fuel has been modified by pressurizing with helium to [ ] and modifying the fuel rods and assemblies in order to accommodate a greater Zircaloy clad growth rate. Changes in the core mechanical design parameters are given in Table 3.1. Additional modifications to the fuel assemblies and an evaluation of the design changes are given in the following core component sections.

3.1.1.1 Fuel Assembly Dimensional Changes

In order to accommodate a higher Zircaloy irradiation growth than was originally anticipated, the fuel assembly dimensions described in the FSAR Figure 3.2.3-9 have been modified to three types of assemblies with dimensional differences. Region 1 has 56 fuel assemblies with the fuel rod lengths reduced to 149.42 inches by using shorter bottom end plugs. The remaining 9 Region 1 fuel assemblies have unchanged fuel rod length, but shorter plate-type bottom nozzles are used. The plate-type nozzles are described in Section 3.1.1.2. Their reference length is 2.738 inches instead of the reference 3.188 inches for the bar-type bottom nozzles. This provides 0.45 inches of additional gap clearance between the fuel rods and nozzles. The new Region 2 and 3 fuel assemblies have fuel rod lengths of 149.37 inches and use the plate-type bottom nozzles. As in Figure 3.2.3-9, Region 1 retains the 144 inch fuel column length, but Regions 2 and 3 have a fuel length of 141.7 inches. The interface of the fuel rods with the plate-type bottom nozzle is shown in Figure 3.1.

As a result of these fuel assembly changes, 56 Region 1 fuel assemblies have a BOL cold fuel rod-nozzle gap of approximately [ ] inches. As burnup accumulates the cold shutdown gap decreases due to irradiation growth of the Zircaloy-clad fuel rods while the stainless-steel thimbles do not grow due to irradiation. Using a conservative design growth rate for irradiated Zircaloy clad fuel rod data (includes upper 2 sigma bound of growth data), analysis of fuel rod growth shows that rod-to-nozzle cold interference (zero gap) is not expected to occur during nominal Cycle 1 exposure, approximately 13,000 effective-full/power-hours (EFPH).

Nine of the 65 Region 1 assemblies have been designed for two cycles of operation by use of the shorter plate-type bottom nozzle. Using the con-servative design growth rate for Zircaloy cladding, fuel rod-to-adaptor plate cold interference is not expected at the nominal EO cycle 2 (21,000 EFPH), due to a larger initial rod-nozzle gap than the other 56 Region 1 assemblies.

Region 2 and 3 fuel assemblies have a BOL cold rod-nozzle gap greater than all the Region 1 assemblies. Using the conservative rod growth design equation, approximately 2 rods per assembly are predicted to be in interference at end of cycle 3 cold shutdown (nominally 29,000 EFPH). In such a case the rods would exert small, acceptable forces on the thimble-nozzle joints.

3.1.1.2 Bottom Nozzle Changes

As stated in the preceeding section, 9 Region 1 and all of the Regions 2 and 3 fuel assemblies use the plate-type bottom nozzles instead of the bar-type described in Section 3.2.3 of the FSAR.*

The bottom nozzle is a box-like structure which serves as a bottom structural element of the fuel assembly and controls the coolant flow distribution to the assembly. The square nozzle is fabricated from type 304 stainless steel and consists of a slotted plate and four angle legs with bearing plates as shown in Figure 3.1. The legs form a plenum for the inlet coolant flow to the fuel assembly.

Coolant flow through the fuel assembly is directed from the plenum in the bottom nozzle upward through the penetrations in the plate to the channels between the fuel rods. The penetrations in the plate are positioned between the rows of the fuel rods.

Axial loads (holddown) imposed on the fuel assembly and the weight of the fuel assembly are transmitted through the bottom nozzle to the lower core plate. Indexing and positioning of the fuel assembly is controlled by alignment holes in two diagonally opposite bearing plate which mate with locating pins in the lower core plate. Any lateral loads on the fuel assembly are transmitted to the lower core plate through the locating pins.

---

*These changes were described previously in a letter dated October 8, 1971, from Consolidated Edison to the AEC. The AEC accepted the new plate-type nozzles as an "equivalent design" in a letter to Consolidated Edison dated February 25, 1972.

3.1.1.3 Fuel Rod Modifications

The description and physical parameters of the fuel rods are given in Section 3.2.3 of the FSAR, except as modified in this section.

Due to Zircaloy growth considerations, the length of most of the fuel rods (all except 9 Region 1 assemblies) have been decreased, as described in Section 3.1.1.1 and shown in Table 3.1. The fuel rod diameter and cladding thickness are unchanged.

To reduce the effects of fuel densification, the fuel pellets in Regions 2 and 3 have been increased to a nominal average density of 95% of theoretical. The Region 2 and 3 pellet diameters have been reduced 1 mil and the pellet-clad diametral gap increased from 6.5 to 7.5 mils. The Region 1 fuel retains its original 94% T.D. and fuel dimensions. The earlier selection of lower fuel densities for Regions 2 and 3 was based upon a conservative interpretation of fuel swelling data. Re-interpretation of this data, as well as new data, indicates that swelling is not as strong a function of density as expected during the three fuel cycles. The higher fuel densities for Regions 2 and 3 for the replacement core will minimize the potential adverse effects of fuel densification which are discussed in Reference 2.

Fuel densification results in the formation of axial fuel column gaps if pellet(s) hangup prevent fuel stack settling. The revised higher fuel densities will minimize the length of such gaps, should they occur. This in combination with Helium prepressurization of all fuel regions assures that clad flattening into potential fuel gaps will not occur during the planned fuel lifetime in the core. The conservative estimates on clad flattening for each fuel region are given in Section 2. The Helium pressurization and fuel density changes necessitates fuel rod design changes in order to satisfy the design basis and criteria stated in Section 3.1 of the FSAR. The fuel rod plenums are sized to assure during normal operation and anticipated transients that the internal rod pressure for the core life of the fuel is less than the nominal 2250 psia coolant pressure. Factors considered in this sizing are the initial Helium pressure, fuel densification, lead burnup and maximum power rods with fuel shuffling for succeeding cycles, and

the effects of design model and manufacturing tolerance uncertainties. The Regions 2 and 3 plenums are increased, which assures the rod internal pressure does not exceed 2250 psia for a "worst-case" analyses using model and tolerance uncertainties. As a result of the requirement for an increased plenum length, the Region 2 and 3 fabricated fuel stacks are reduced from the original 144 to 141.7 inches. The Region 1 fuel stack dimensions are unchanged, since the Region 1 plenum length is sufficient to prevent exceeding 2250 psia rod pressure during cycle 1 for the worst-case analyses. If used during all of cycle 2, it is predicted that Region 1 fuel rods would not exceed 2250 psia internal pressure based on a best-estimate analysis (excluding model and tolerance uncertainties).

3.1.2 NUCLEAR DESIGN

Major design changes that affect the nuclear characteristics of IPP-2 are the enrichment, density and initial pressurization. These parameters are shown in Table 3.2. The regionwise fuel loading pattern remains unchanged and is shown in Figure 3.2. In order to accommodate the higher enrichments and to meet the power peaking design requirements the number of burnable poison rods had to be increased from 1160 to 1412 and the pattern revised. Figure 3.3 illustrates the revised poison rod pattern by assembly.

In addition the nuclear enthalpy rise hot channel factor, $F^N_{\Delta H}$, has been reduced to 1.65 and the total heat flux design factor has been reduced to 2.70, which includes the engineering factor, F^E_q, of 1.03. The original $F^N_{\Delta H}$ was conservative and has been reduced in line with current technology. The revised F^{tot}_q has been derived by considering all allowable operating situations and the effects of densification. These factors along with other nuclear design data are tabulated in Table 3.3. Tables 3.4 and 3.5 are also enclosed which show control rod reactivity requirements and worths.

References for Section 3

1. "Final Facility Description and Safety Analysis Report - Indian Point Nuclear Generating Unit No. 2," Docket No. 50-247.

2. Eng, G., et al., "Fuel Densification Penalty Model," WCAP-7984, October, 1972.

TABLE 3.1

CORE MECHANICAL DESIGN PARAMETERS[1]

Active Portion of the Core	
Equivalent Diameter, in.	132.7
Active Fuel Height, in.	144.0 R1, 141.7 R2/R3[2]
Length-to-Diameter Ratio	1.09
Total Cross-Section Area, Ft^2	96.06
Fuel Assemblies	
Number	193
Rod Array	15 x 15
Rods per Assembly	204
Rod Pitch, in.	0.563
Overall Dimensions	8.426 x 8.426
Fuel Weight, (as UO_2), pounds	217,800
Total Weight, pounds	273,000
Number of Grids per Assembly	9
Number of Guide Thimbles	20
Diameter of Guide Thimbles (upper part), in.	0.545 O.D. x 0.515 I.D.
Diameter of Guide Thimbles (lower part), in.	0.484 O.D. x 0.454 I.D.
Fuel Rods	
Number	39,372
Outside Diameter, in.	0.422
Diametral Gap, in.	0.0065 R1; 0.0075 R2/R3
Clad Thickness, in.	0.0243
Clad Material	Zircaloy
Region 1 Overall Length, in.	149.6/149.4 (9/56 F. Ass.)[3]
Region 1 Length of Bottom End Cap, overall, in.	0.688/0.488 (9/56 F. Ass.)
Region 1 Length of Top End Cap, overall, in.	0.688
Region 1 Length of Top and Bottom Caps, inserted in rod, in.	0.250
Region 2 & 3 Overall Length, in.	149.4
Region 2 & 3 Length of Top and Bottom End Caps, overall, in.	.688/.502 (Top/Bottom)
Region 2 & 3 Length of End Cap, inserted, in.	.250
Fuel Pellets	
Material	UO_2 sintered
Density (% of Theoretical)	
Region 1	94 (10.3 g/cc)
Region 2	95 (10.4 g/cc)
Region 3	95 (10.4 g/cc)
Feed Enrichments w/o	
Region 1	2.2
Region 2	2.8
Region 3	3.3
Diameter, in.	0.3669 R1, 0.3659 R2/R3
Length, in.	0.600

TABLE 3.1 (Cont'd)

Rod Cluster Control Assemblies	
Neutron absorber	5% Cd, 15% In, 80% Ag
Cladding Material	Type 304 SS - Cold Worked
Clad Thickness, in.	0.019
Number of Clusters	
Full Length	53
Part Length	8
Number of Control Rods per Cluster	20
Length of Rod Control, in.	156.436 (overall)
	149.136 (insertion length)
Length of Absorber Section, in.	142.00 (full length)
	36.00 (part length)
Core Structure	
Core Barrel, in.	
I.D.	148.0
O.D.	152.5
Thermal Shield, in.	
I.D.	158.5
O.D.	164.0
Burnable Poison Rods	
Number	1412
Material	Borosilicate Glass
Outside Diameter, in.	0.4395
Inner Tube, O.D., in.	0.2365
Clad Material	S.S.
Inner Tube Material	S.S.
Boron Loading (natural) gm/cm of glass rod	0.0429

(1) All dimensions are for cold conditions.

(2) R1 = Region 1; R2/R3 = Regions 2 and 3.

(3) 9/56 F. Ass.: First tabulated valve is for 9 fuel assemblies, second tabulated valve is for 56 fuel assemblies in Region 1.

TABLE 3.2

FUEL ASSEMBLY DESIGN PARAMETERS

Region	1	2	3
Enrichment	2.2	2.8	3.3
Geometric density (% theoretical) - as built region average	93.6	*	*
Initial Helium pressurization (psia)	[		]

* As built values not available for Regions 2 and 3 at time of analysis; therefore, 94.3% assumed for this evaluation of densification effect for the specified design value of 95%.

TABLE 3.3

NUCLEAR DESIGN DATA

STRUCTURAL CHARACTERISTICS

1.	Fuel Weight (UO_2), lbs.	217,800
2.	Zircaloy Weight, lbs.	44,600
3.	Core Diameter, inches	132.7
4.	Active Fuel Height, inches	144 (Region 1)
		141.7 (Regions 2 and 3)
	Reflector Thickness and Composition	
5.	Top - Water Plus Steel	∿ 10 in.
6.	Bottom - Water Plus Steel	∿ 10 in.
7.	Side - Water Plus Steel	∿ 15 in.
8.	H_2O/U, (Cold) Core	4.16
9.	Number of Fuel Assemblies	193
10.	UO_2 Rods per Assembly	204

PERFORMANCE CHARACTERISTICS

11.	Heat Output, MWt (initial rating)	2758
12.	Heat Output, MWt (maximum calculated turbine rating)	3216
13.	Fuel Burnup, MWD/MTU	16,700
	First Cycle	
	Enrichments, w/o	
14.	Region 1	2.2
15.	Region 2	2.8
16.	Region 3	3.3
17.	Equilibrium Enrichment	3.2
18.	Nuclear Heat Flux Hot Channel Factor, F_Q^N	2.62
19.	Nuclear Enthalpy Rise Hot Channel Factor, $F_{\Delta H}^N$	1.65

TABLE 3.3 (Cont'd)

CONTROL CHARACTERISTICS

	Effective Multiplication (Beginning of Life) with Rods in; No Boron	
20.	Cold, No Power, Clean	1.12
21.	Hot, No Power, Clean	1.06
22.	Hot, Full Power, Clean	1.04
23.	Hot, Full Power, Xe and Sm Equilibrium	1.01
24.	Material	5% Cd; 15% In; 80% Ag
25.	Full Length	53
26.	Partial Length	8
27.	Number of Absorber Rods per RCC Assembly	20
28.	Total Rod Worth, BOL, %	(See Table 3.4)
	Boron Concentration for First Core Cycle Loading With Burnable Poison Rods	
29.	Fuel Loading Shutdown; Rods in (k = .90)	1615 ppm
30.	Shutdown (k = .99) with Rods Inserted, Clean, cold	900 ppm
31.	Shutdown (k = .99) with Rods Inserted, Clean, Hot	625 ppm
32.	Shutdown (k = .99) with No Rods Inserted, Clean, Hot	1455 ppm
33.	Shutdown (k = .99) with No Rods Inserted, Clean, Cold	1420 ppm
	To Maintain k = 1.0 at Hot Full Power, No Rods Inserted:	
34.	Clean, BOL	1210 ppm
35.	After 100 EFPH	930 ppm
36.	Shutdown, All But One Rod Inserted, Clean Cold (k = .99)	965 ppm
37.	Shutdown, All But One Rod Inserted, Clean Hot (k = .99)	730 ppm

TABLE 3.3 (Cont'd)

BURNABLE POISON RODS		
38.	Number and Material	1412 Borated Pyrex Glass
KINETIC CHARACTERISTICS		
39.	Moderator Temperature Coefficient At Full Power ($°F^{-1}$)	$-.35 \times 10^{-4}$ to -3.25×10^{-4}
40.	Moderator Pressure Coefficient (psi^{-1})	$+.2 \times 10^{-6}$ to $+3.00 \times 10^{-6}$
41.	Moderator Density Coefficient, $\Delta k/gm/cm^3$	-.1 to .30
42.	Doppler Coefficient ($°F^{-1}$)	-1.1×10^{-5} to -1.8×10^{-5}
43.	Delayed Neutron Fraction, %	.50 to .70
44.	Prompt Neutron Lifetime, sec.	1.9×10^{-5}

TABLE 3.4

REACTIVITY REQUIREMENTS FOR CONTROL RODS

Requirements	Per Cent $\Delta\rho$ Beginning of Life	End of Life
Control		
Power Defect	1.54	2.10
Rod Insertion Allowance	.70	.70
Void	.08	.08
Redistribution	.30	.85
Total Control	2.62	3.73

TABLE 3.5

CALCULATED ROD WORTHS, $\Delta\rho$

Core Condition	Rod Configuration	Worth	Less 10%*	Design Reactivity Requirements	Shutdown Margin
BOL, HFP	53 rods in	9.77%			
	52 rods in; Highest Worth Rod Stuck Out	8.27%	7.44%	2.62%	4.82%
EOL, HZP (1st Cycle)	53 rods in	8.76%			
	52 rods in; Highest Worth Rod Stuck Out	7.28%	6.55%	3.73%	2.82%**

BOL = Beginning of Life

EOL = End of Life

HFP = Hot Full Power

HZP = Hot Zero Power

* Calculated rod worth is reduced by 10% to allow for uncertainties.

** The design basis minimum shutdown margin is 1.95%.

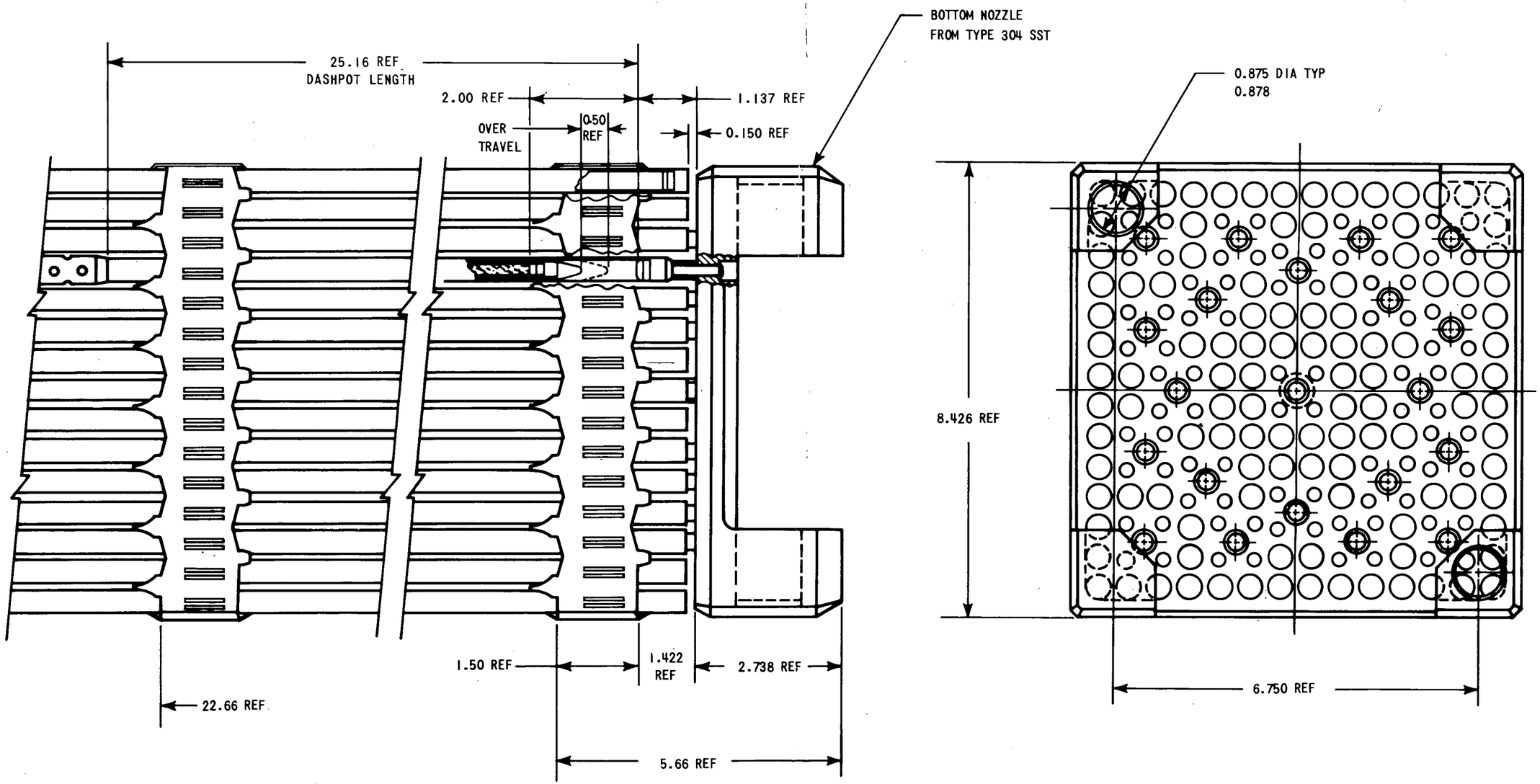

Figure 3.1. Bottom End of Fuel Assembly Showing Plate Type Bottom Nozzle

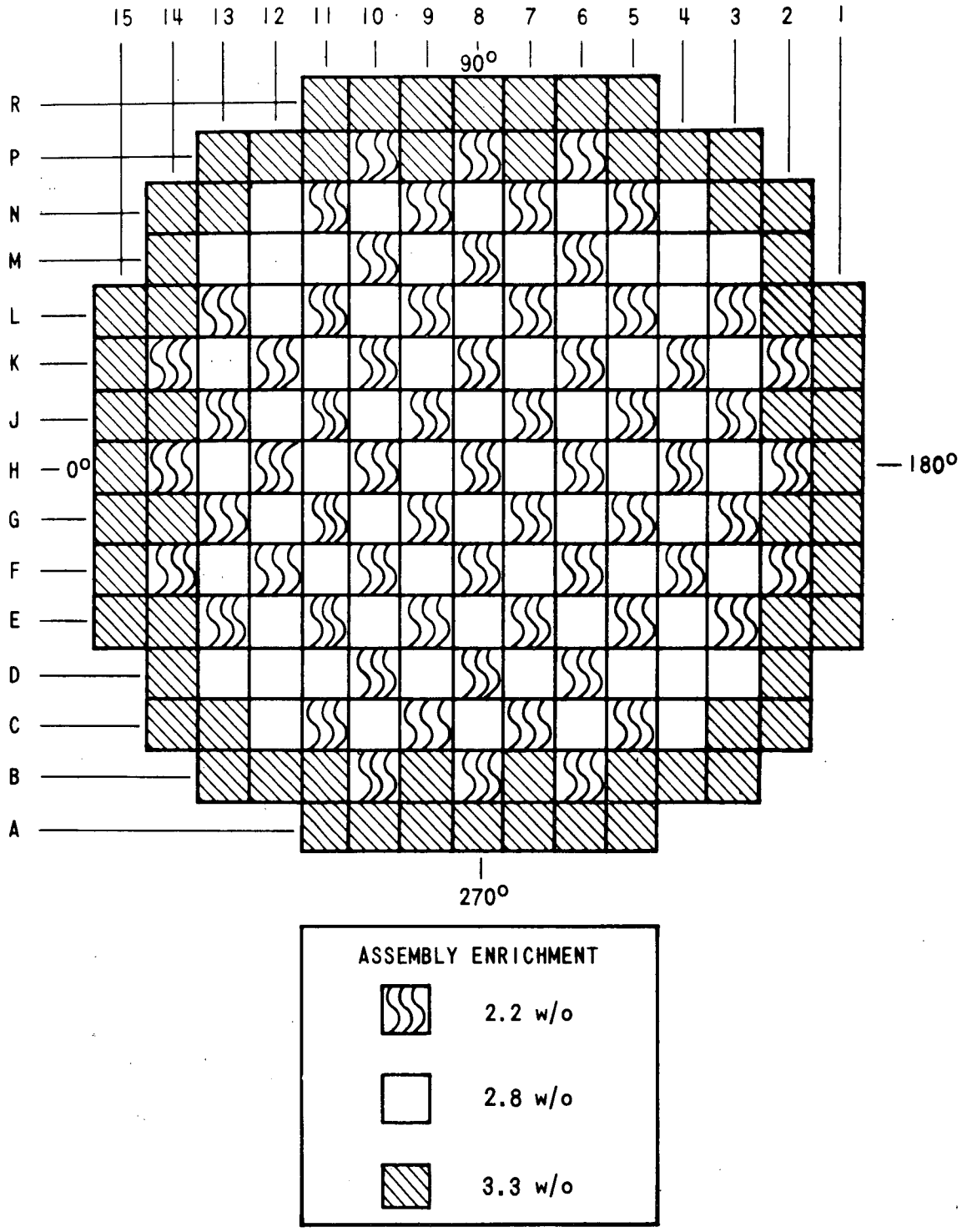

Figure 3.2. Fuel Loading Diagram Indian Point Unit No. 2 Cycle 1

FIGURE 3.3

BURNABLE POISON PATTERN

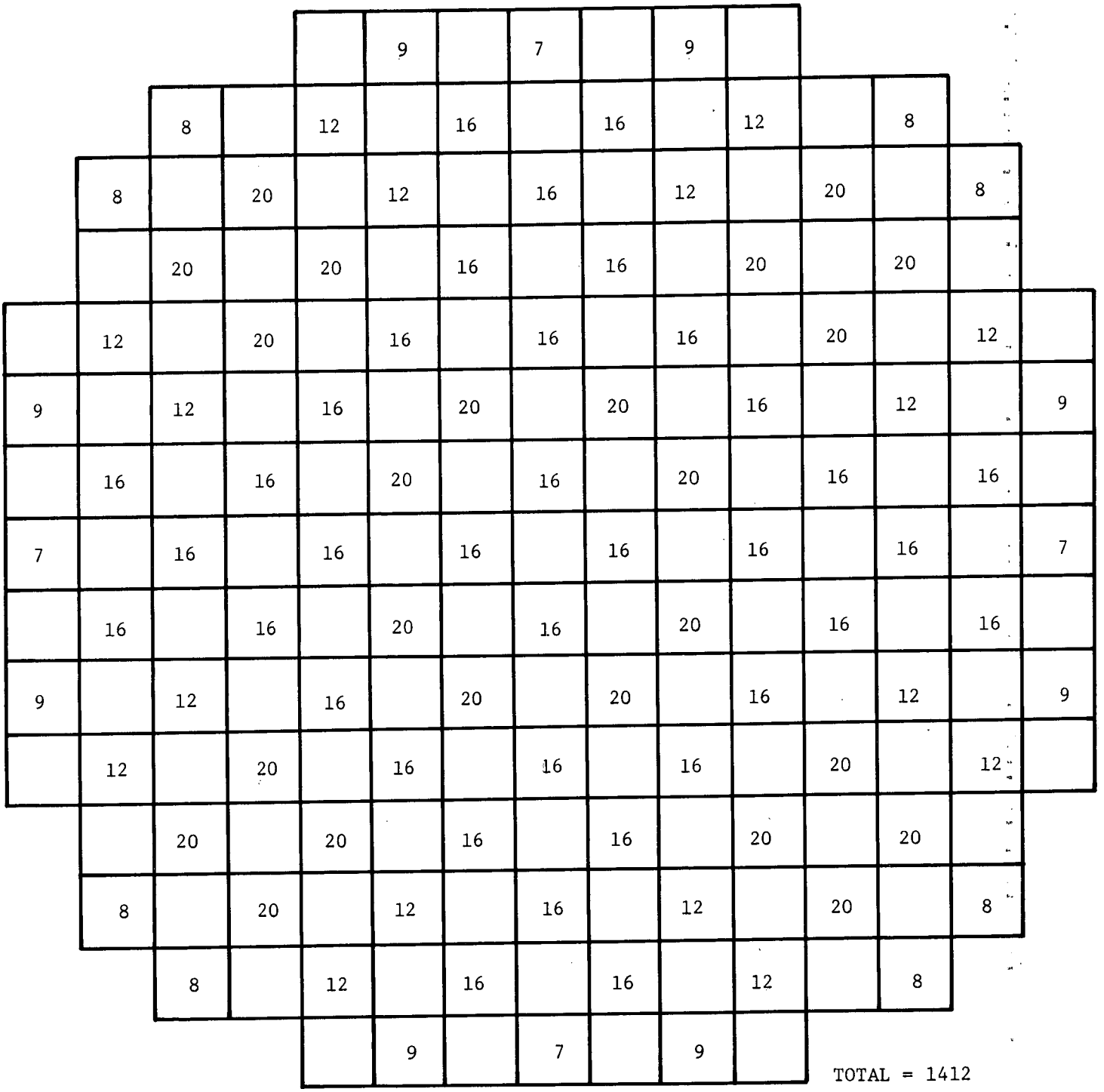

TOTAL = 1412

4.0 FUEL PERFORMANCE LIMITS

4.1 LOCAL POWER PEAKING DUE TO FUEL DENSIFICATION

For the purpose of re-evaluating fuel performance limits including the effects of fuel densification on local power peaking, a series of conservative assumptions have been made. These are based on visual observation of fuel clad flattening and on in-core flux traces in the Beznau, R. E. Ginna, Point Beach 1 and H. B. Robinson reactors. The data on which these assumptions are based and the methods of determining local power peaking due to gaps in the fuel column are given in detail in WCAP-7978[1]. The major assumptions for determining local power peaking are:

a) For the purpose of determining acceptable operation it has been conservatively assumed that full fuel pellet densification takes place at zero burnup.

b) The local power peaking effect is calculated with the following assumptions relative to the characteristics of axial gaps:

1. All fuel rods are subject to densification.

2. The frequency distribution of gaps by axial position is based on in-core flux traces from Point Beach 1 and H. B. Robinson. It is assumed that the frequency of occurrence of significant gaps increases linearly with height from the bottom of fuel.

3. The distribution of gap size is based on rod flattening observed in the R. E. Ginna reactor between the 120 in. and 140 in. elevations. This distribution is the same as that recommended by the AEC in their "Technical Report on Densification of Light Water Reactor Fuels".[2]

4. The maximum size for a gap increases linearly with height from the bottom of fuel (H) according to

$$\left(\frac{0.965-\rho}{2} + 0.004\right) H$$

where ρ is the initial density of the fuel.

5. The distribution of gap size at any elevation is the distribution from (3) with the scale multiplied by the appropriate factor to produce a maximum gap size equal to that given by (4).

d) The criterion chosen for an acceptable design value of power peaking due to fuel densification, including the power spike, is that less than one fuel rod will exceed F_Q^N at a 95% confidence level.

The local peaking due to gaps in the fuel column as a function of axial position has been calculated for the Indian Point Unit 2 reactor - Cycle 1 and the results are given in Figure 4.1.

4.2 TOTAL POWER PEAKING FACTOR, F_Q

Since the magnitude of the local power peaking varies as a function of height in the core, it has been applied to the basic power shape data which determines the design value of F_Q. The basis for protection against exceeding local power density limits is given in topical reports which describe the use of excore detector signals (axial offset) in the over-power protection logic.

An upper bound on F_Q is set as a function of axial offset by consideration of all allowable operating situations. When F_Q is increased locally by the height dependent local power peaking, the individual points are increased in F_Q by different amounts. The result is a revised plot of F_Q vs. axial offset which requires a revised upper bound different in shape and magnitude from the previous upper bound.

For the fuel cycle under consideration, the results are given in Figure 4.2 which incorporates the flux peaking penalty of Figure 4.1. Figure 4.2 also includes a 5% margin for uncertainty and 3% for manufacturing tolerances. In the calculations it was assumed that the horizontal peaking factor, F_{xy}, at the plane of the peak local power was no lower than 1.44. A high F_Q could occur as a result of control rod insertion to the control rod insertion limits in the Technical Specification. For this reason, the plot contains points at large axial offset evaluated for less than full power, with an F_{xy} appropriate to the plane of the peak F_Q. An additional operating limit is that no part length control rods are permitted in the bottom third of the core at full power. The boundary is used to define protection set points and operating limits for all conditions. The figure indicates that a total peaking factor, F_Q, of 2.70 can be maintained by reference only to the ex-core detector axial offset.

4.3 THERMAL AND HYDRAULIC PARAMETERS

Table 4.1 presents a summary of the pertinent design parameters which have been changed from those presented in the FSAR. An explanation or description of each change is presented below.

a) $F^N_{\Delta H}$ has been reduced from 1.75 to 1.65 in order to provide additional margin for DNB to offset the penalty for fuel densification. This is discussed in Section 3.1.2.

b) F_Q has been decreased to 2.70. This allows for local power peaking due to fuel densification. This is discussed in Section 4.2.

c) The reference axial power distribution for DNB analysis has been changed from a chopped cosine with a 1.79 peak to one with a 1.55 peak. This has an impact on the permissible range of axial offset under normal operating conditions and is reflected in the overtemperature ΔT protection set points. The tighter control of power distribution that is required for DNB protection is not inconsistent with the restrictions already imposed by operation to meet the revised peak power density limits.

d) Based on Westinghouse latest rod bundle DNB data, the W-3 DNB correlation for both a typical cell (all channel walls heated) and a thimble cell (partial channel walls heated) is applied in the present analysis. (See Section 4.5)

e) F^E_Q for DNB evaluations has been increased from 1.03 to 1.05 due to fuel densification considerations. Fuel pellet shrinkage increases the fuel/clad gap and the factor to account for non-uniform azimuthal heat flux. This non-uniform flux is caused by the clad developing an ovality and contacting the pellet at two points. Reduced fuel rod circumference and heat transfer area is also considered in the value.

f) The fuel densities differ from the FSAR values. For Regions 2 and 3, the analysis assumes a geometric density is 94.3% for the nominal design value of 95%. For Region 1, the as-built density 93.6% is employed in place of the design value of 94%.

g) The core average active fuel height and heat transfer surface area have been revised to include i) the new design values for the fuel stack height as described in Section 3.1.1.3 and ii) the effect of core average pellet densification and thermal expansion.

4.4 EFFECT OF FUEL DENSIFICATION ON FUEL TEMPERATURES

In addition to the local power peaking, fuel densification may result in an increase in the radial gap between the fuel and the clad, leading to a decrease in gap conductance and an increase in fuel temperature. Densification also leads to an increase in linear heat generation rate due to the reduction in the fuel length. Later in life, the cladding creeps down onto the fuel and the heat transfer performance of the fuel is improved.

Fuel column length changes have been measured by gamma scan as discussed in Reference 3. The reduction in pellet stack height conservatively determined from these data is used in the determination of the linear heat generation rate. That is

$$\frac{\Delta L}{L} = \frac{0.965-\rho}{2}$$

where ρ is the initial density of the fuel.

The densification of the fuel pellet is assumed to occur immediately and the effect of the resulting increase in the fuel-clad gap on the fuel centerline and average fuel temperature was determined with the models discussed in Reference 3.

Calculations of the linear power increase and of the fuel temperature, with densification, utilize the as-fabricated average density of the Region 1 fuel. This is the lowest density and most limiting region in the core.

The effect of the statistical variations in the pellet density on the densified pellet length and radius are accounted for by increasing the power spike used in the temperature calculations. This is done by including equivalent thermal effects of pellet density variations in the probability analysis for the power spike as described in Reference 1. The evaluation is based on; (a) the spike probability and the x-y power census as presented

in Reference 1 with modifications per Reference 2, (b) the variability in the pellet density obtained from Region 1 pellet density measurements, and (c) the relationship between a change in initial fuel density and the associated change in the loss of coolant linear power limit, or in the thermal overpower limit.

This analysis results in the power peaking being increased 0.7% for loss of coolant evaluations and 2.0% for thermal overpower evaluations. The methods used in the probability calculation provide a confidence level of 95% that the actual power peaking in the reactor core will not exceed the maximum calculated peaking for more than one rod in the core. The values are different for LOCA and overpower because of different ratios of power limit to initial density variation [Item (c) above].

The criteria for overpower transients is that fuel pellet centerline melting will not occur. In addition, peak fuel rod power is not permitted to exceed 21.1 kw/ft during an overpower transient.

Figures 4.3 and 4.4 give the results of fuel centerline and fuel average temperature calculations as a function of burn-up for the most limiting region, that is, Region 1 with the lowest density fuel. The calculation of clad creep was for a fuel rod in that region having low burnup, thereby, the clad creep rate and associated temperature reduction are minimized.

A temperature limit of 4700°F is applied for the first several thousand hours of operation when centerline temperature can be limiting. The difference between this value and the UO_2 melting temperature (5080°F at BOL and decreasing by 58°F per 10,000 MWD/MTU) provides margin for uncertainties in the evaluation.

As seen in Figure 4.3, the limit of 21.1 kw/ft is reached slightly before a fuel centerline temperature of 4700°F is attainable.

4.5 DNB EVALUATION

4.5.1 HIGH PRESSURE DNB DATA

With the conclusion of the Westinghouse ESADA DNB program[4], where data was obtained from rod bundle geometries, mixing vane grids, non-uniform axial heat flux distributions and pressures from 1490 to 2400 psia, Westinghouse has removed an uncertainty factor which was applied to the W-3 correlation previously used in all reactor designs, including that presented in the FSAR for the Indian Point Power Station. This factor was applied for conservatism because of the small amount of DNB data previously available at higher reactor operating pressures.

4.5.2 Definition of DNB Heat Flux Ratio

The DNB heat flux ratio as applied to this design when all flow cell walls are heated is

$$DNBR = \frac{q''_{DNB,N}}{q''_{loc}} \tag{1}$$

where

$$q''_{DNB,N} = \frac{q''_{DNB,EU}}{F} \tag{2}$$

and $q''_{DNB,EU}$ is the uniform DNB heat flux as predicted by the W-3 DNB correlation[5] when all flow cell walls are heated.

F is the flux shape factor to account for nonuniform axial heat flux distributions[5] with the "C" term modified as in Reference (6).

q''_{loc} is the actual local heat flux.

The DNB heat flux ratio as applied to this design when a cold wall is present is

$$DNBR = \frac{q''_{DNB,N,CW}}{q''_{loc}} \tag{3}$$

where

$$q''_{DNB,N,CW} = \frac{q''_{DNB,EU,Dh} \times CWF}{F} \tag{4}$$

where

$q''_{DNB,EU,Dh}$ is the uniform DNB heat flux as predicted by the W-3 cold wall DNB correlation[7] when not all flow cell walls are heated (thimble cold wall cell).

$$CWF^{(7)} = 1.0 - Ru\ [13.76 - 1.372e^{1.78x} - 4.732\ (\frac{G}{10^6})^{-.0535} - .0619\ (\frac{P}{1000})^{.14} - 8.509Dh^{.107}] \tag{5}$$

and $Ru = 1 - De/Dh$

4.5.3 F-Factor Evaluation

The W-3 DNB correlation includes a factor to account for axially nonuniform heat fluxes.[8]

An evaluation of the ability of this factor to predict DNB behavior of short heat flux spikes was done by comparing the measured DNB heat fluxes from two experimental test sections[9,10] to that calculated. The mean of the measured to predicted evaluations was 0.98. The scatter of the points about the mean was +18, -14 percent. No trends within the scatter were noted, and it was concluded that the non-uniform factor in the W-3 adequately describes the DNB behavior of heat flux spikes.

4.5.4 DNB Method

The DNB evaluation method with densification is summarized in Table 4.2. For all analyses the power peak and engineering hot channel factor described previously are applied at the axial location of minimum DNBR.

The heat flux spike shape, i.e., axial heat flux distribution in a given fuel rod, is the sum of the contribution of fuel pellet separation in neighboring rods within three rows of that rod. An examination of combinations of gap positions that would lead to the largest power spike was made. From this evaluation the combination of gaps was selected that resulted in the largest power spike over the greatest fuel rod length. This in turn gives the maximum DNB penalty.

The magnitude of the power spike used for DNB purposes is conservatively assumed to be the magnitude of the spike 4 inches from the top of the core. In other words, flux shapes which lead to a minimum DNBR in the top 4" of the fuel rod do not occur. A conservative trapezoidal approximation to the heat flux spike has been developed for DNB purposes and is applied at the point of minimum DNBR.

The standard DNB evaluation method (THINC I code) has been modified to evaluate the DNBR including the power spike. The reduction in active pellet height due to densification is considered by increasing linear heat generation rate by a factor of 1.02. Consideration of the "as fabricated" fuel length and axial thermal expansion as well as the densification are included in the evaluation.

Core DNB limits have been determined based on the design parameters listed in Section 4.3 and the DNB method outlined in Section 4.5.2. The results are given in terms of core power and T_{avg} limits in Section 5.3.

References for Section 4

1) George, R. A., W. D. Leggett III, "Power Spike Model", WCAP-7978, October 1972.

2) "Technical Report on Densification of Light Water Reactor Fuels", Regulatory Staff U.S.A.E.C., November 14, 1972.

3) Eng. G., et. al., "Fuel Densification Penalty Model", WCAP-7984, October 1972.

4) Rosal, E. R., J. O. Cermak, L. S. Tong, "Rod Bundle Axial Non-Uniform Heat Flux DNB Tests and Data", WCAP-7411-L Rev. I, May 1970, Westinghouse Proprietary Class II.

5) Tong, L. S., "Prediction of Departure from Nucleate Boiling for an Axially Non-Uniform Heat Flux Distribution", J. Nul. Energy, 21, pp. 241-248, 1967.

6) Trojan PSAR, Portland General Electric Co., Docket 50-344.

7) Tong, L. S., "Boiling Crisis and Critical Heat Fluxes", AEC Critical Review Series, TID-25887, 1972.

8) Tong, L. S., H. B. Currin, P. S. Larsen and O. G. Smith, Chemical Engineering Progress Symposium Series, Vol. 62, Number 64, 1966.

9) Styrikovich, M. A., R. L. Miropol'skii and V. K. Eva, "The Influence of Local Raised Heat Fluxes Along the Length of the Channel on the Boiling Crises", Soviet Physics Doklady, Vol. 7, 1963.

10) Weiss, A., "Hot Patch Burnout Test on a 0.097 inch x 1.0 inch x 27 inch Long Rectangular Channel at 2000 psia", WAPD-TH-388, 1957.

TABLE 4.1

COMPARISON OF THERMAL DESIGN PARAMETERS

	FSAR	Present Supplement
Nuclear Enthalpy Rise Hot Channel Factor for DNB evaluation, $F^N_{\Delta H}$ (ratio of the integral of the heat generation rate within the hottest rod to the heat generation rate in the average rod including an uncertainty factor.)	1.75 (10% uncertainty)	1.65 (10% uncertainty)
Total heat flux hot channel factor, F_Q (ratio of maximum core heat flux to average core heat flux)	3.00 (Interim Acceptance Criteria)*	2.70 (Includes densification penalty)
Heat flux engineering hot channel factor, F^E_Q		
a) kw/ft evaluation	1.03	1.03
b) DNB evaluation	1.03	1.05
Reference axial power distribution for DNB Evaluation	1.79 chopped cosine	1.55 chopped cosine
Region Densities, Geometric, %		
Region I	94	93.6
Region II	92	94.3
Region III	91	94.3
Core Average Active Fuel Height, inches	144.0	141.5
Heat transfer surface area, ft^2	52,200	51,300
DNB Correlation	W-3	W-3
Minimum DNBR for DNB core safety limits	1.30	1.30

* Presented in "Additional Testimony of Applicant Concerning Emergency Core Cooling System Performance", July 13, 1971, Docket No. 50-247.

TABLE 4.2

DNB EVALUATION METHOD

Local power peaking due to fuel column gaps is applied at location of minimum DNBR for all steady state and transient evaluations.

Heat flux increase due to total fuel pellet stack height reduction is included.

Maximum length of local power spikes is used.

Additional hot channel factor due to increased pellet-clad eccentricity is applied, 1.019.

Standard DNB evaluation methods (THINC Code) have been modified to include above effects and are used in analysis.

FIGURE 4.1

POWER SPIKE FACTOR VS ELEVATION

IPP2, CYCLE 1

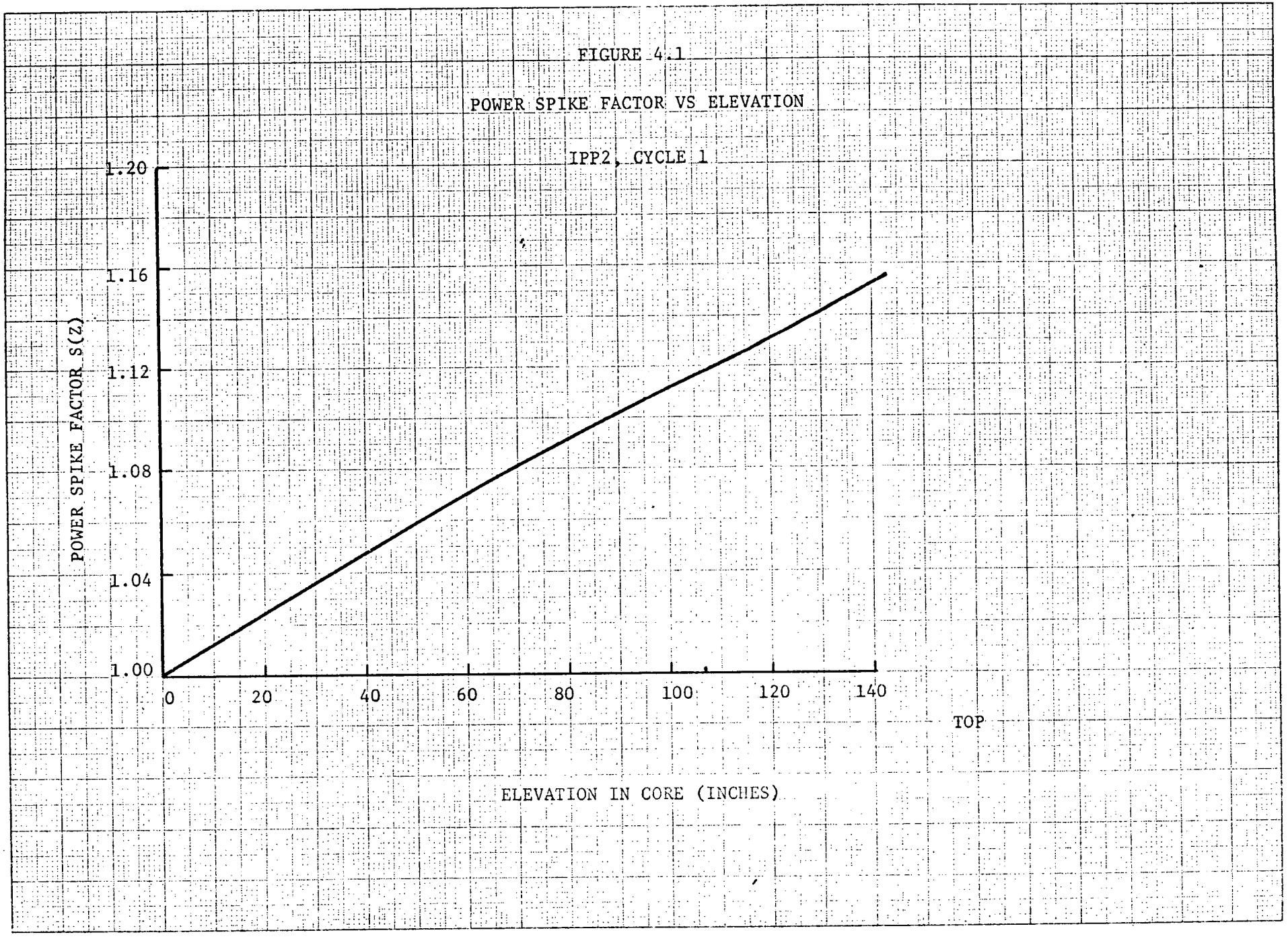

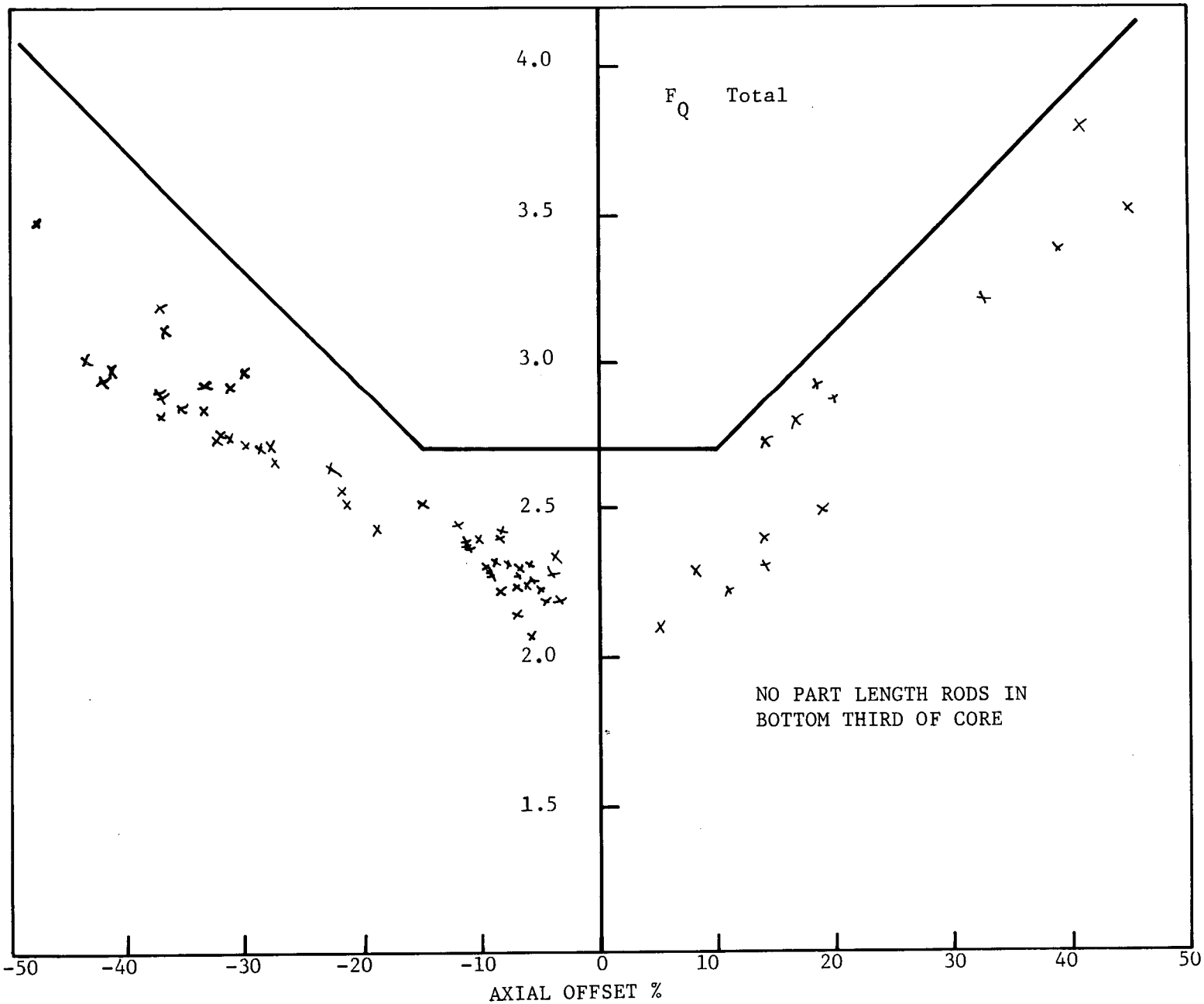

Figure 4.2 TOTAL HEAT FLUX PEAKING FACTOR - F_Q VS AXIAL OFFSET

FIGURE 4.3

INDIAN POINT UNIT 2
REGION 1
MINIMUM BURNUP ROD
WITH DENSIFICATION
FUEL CENTERLINE TEMPERATURE
VS
ROD POWER AT VARIOUS OPERATING TIMES

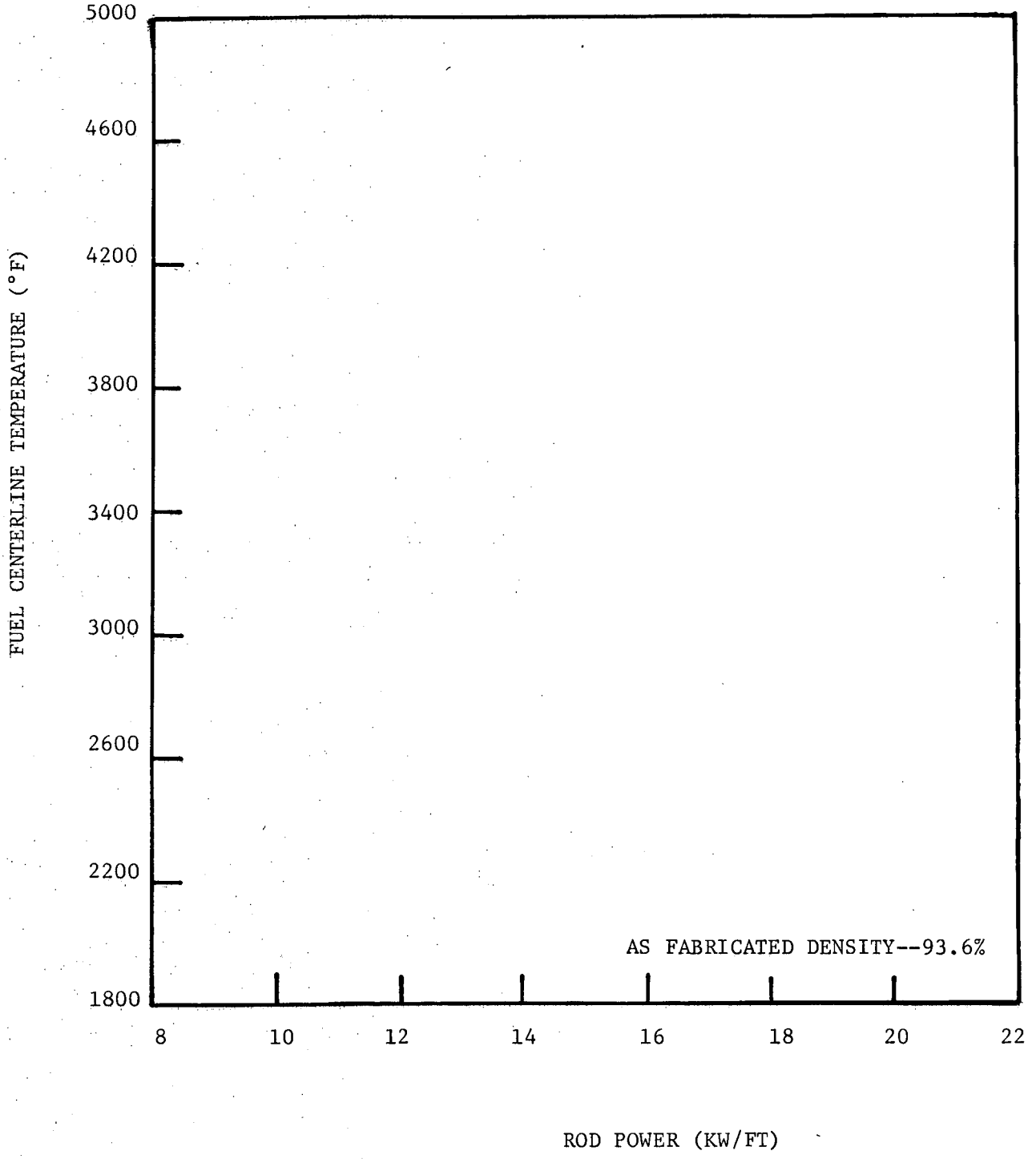

FIGURE 4.4

INDIAN POINT UNIT 2
REGION 1
MINIMUM BURNUP ROD WITH DENSIFICATION
FUEL AVERAGE TEMPERATURE
VS
ROD POWER AT VARIOUS OPERATING TIMES

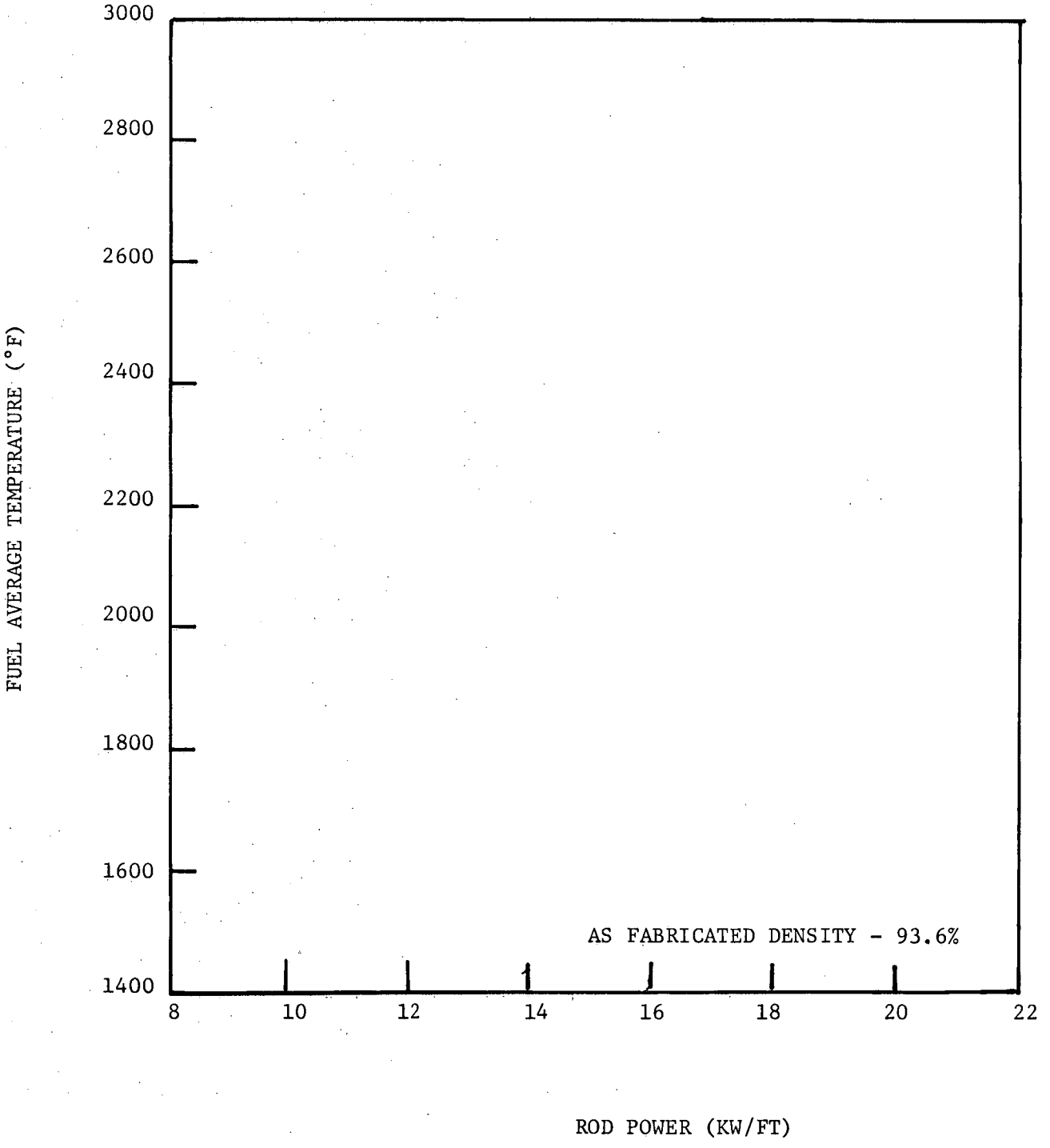

5.0 POWER CAPABILITY

5.1 GENERAL

The effects associated with fuel densification can be separated into three categories as below:

1) Reduction in pellet stack height due to densification. This effect increases the average linear rod heat flux by an amount equivalent to the percentage reduction in pellet stack height.

2) Power spikes caused by axial gaps in a fuel rod and in surrounding rods. This effect increases core peaking factors by the value of the power spike.

3) Increase in pellet-cladding gap due to radial densification. This effect increases fuel pellet temperatures.

The first two of these effects cause an increase in local rod power (kw/ft). The third effect causes, as noted, higher pellet temperatures and thus increases stored energy in the fuel.

These three phenomena have some effect on most of the design bases transients and postulated accidents analyzed in the FSAR. However, the effects of fuel densification can be accommodated in the design and operation of Indian Point Unit No. 2 without any loss of power capability. For some transients, the penalties incurred may be absorbed without requiring additional restrictions on operation to meet design basis criteria. These transients are discussed in Section 6. The types of incidents which are most inclined to impose restrictions on operation are those involving overpower transients, those affecting DNB safety limits, and the Loss of Coolant accident and are addressed here in Section 5. The requirements imposed to meet design basis criteria for these incidents thus determine plant power capability. These requirements are discussed below.

5.2 OVERPOWER TRANSIENT LIMITS

The criterion for overpower protection requires that the maximum fuel temperature be limited to a value less than the fuel centerline melting temperature for normal operation and anticipated transients. This protection is provided by the Overpower ΔT trip and the nuclear overpower trip. As a basis for establishing overpower protection system setpoints, a calculated centerline fuel temperature of 4700°F has been selected as the overpower limit. In addition, peak fuel rod power is not permitted to exceed 21.1 kw/ft during an overpower transient.

Fuel centerline temperatures have been calculated for the most limiting region (Region 1) as a function of local linear power and fuel burnup using the methods discussed in Section 4; these results are shown on Figure 4.3.

Considering the effect of radial fuel densification on fuel temperature at BOL the maximum centerline temperature at the design overpower limit of 21.1 kw/ft is 4640°F.

To provide margin for operation and allowance for instrument errors, the maximum overpower limit should be about 20% of rated power greater than the allowable operating power. For this core with a total peaking factor F_Q of 2.70 (as discussed in Section 4.2) the maximum overpower limit at BOL is:

$$\text{Maximum overpower limit} = \frac{21.1}{5.7 \times 1.02 \times 2.7 \times 1.02} = 131.8\%$$

where the factors above include a 2% allowance for axial fuel stack height change from the design value (due to shrinkage and thermal expansion) which is a direct multiplier on the average linear rod power at rated power, and an additional 2% allowance for the effect of local pellet density variations on fuel centerline temperatures as discussed in Sec. 4.4.

Since fuel centerline temperatures for a given linear rod power decrease with burnup due to clad creep down, the BOL conditions are the most restrictive with respect to overpower transient limits. Since the transient overpower limit is 131.8% of rated power, the margin to this limit is more than sufficient to allow operation at full rated power.

5.3 DNB LIMITS

5.3.1 DNB CORE SAFETY LIMITS

The criterion for DNB protection requires that the minimum DNBR will be no less than 1.30 for normal operation and anticipated transients. The primary DNB protection is provided by the Overtemperature ΔT trip.

The DNB core safety limits have been recalculated to allow for the effects of fuel densification. The recalculation of these limits includes DNB penalties for increased pellet eccentricity, local power spikes, local pellet density variations, 10% uncertainty in $F_{\Delta H}^{N}$, a reference cosine with a peak of 1.55 for axial power shape, and current DNB technology as discussed in Section 4.

The recalculated DNB core safety limits have been found to be less limiting than those previously presented in the FSAR, i.e. the reduction in design peaking factors more than offsets the effects of fuel densification on the DNB Ratio. Thus the DNB core limits are adequate and conservative as presented in the FSAR and the Overtemperature ΔT reactor trip setpoints need not be revised.

5.3.2 DNB PROTECTION ANALYSIS

The loss of reactor coolant flow accident is a rapid transient which is not terminated by the Overtemperature ΔT trip. This transient has been analyzed on a conservative basis and it has been determined that the limiting criteria of DNBR $\geq$ 1.30 is met for the worst case. The analysis performed for the loss of reactor flow and other incidents is discussed in detail in Section 6.

5.4 LOSS OF COOLANT ACCIDENT LIMITS

The Westinghouse evaluation model has been utilized to evaluate the effects of fuel densification on the LOCA transient in accordance with the requirements of the Interim Policy Statement.

The limiting criterion is the limit on peak clad temperature, i.e. 2300°F. As shown by core cooling analysis presented in the FSAR, the worst break is the double-ended cold leg guillotine and this break has been reanalyzed considering the effects of fuel densification. The blowdown transient (SATAN code) was calculated at 102% of rated core power. The fuel temperature calculations were made with the LOCTA code at various initial hot spot pellet average temperatures to determine the maximum allowable linear rod power. The loci of initial pellet average temperature and kw/ft which meet the Emergency Core Cooling System criteria are shown in Figure 5.1. Figure 5.1 also shows the calculated average fuel rod temperature for Region 1 with densified fuel versus kw/ft at various values of fuel burnup determined as described in Section 4. The average fuel temperature decreases with reactor operation because of clad creep down and consequently higher peak local rod power is acceptable with increased burnup.

From Figure 5.1, the maximum linear rod power which meets the ECCS criteria at beginning of life is 17.35 kw/ft. The maximum linear rod power for operation at full rated power is

$$5.7 \times 1.02 \times 1.02 \times 2.70 \times 1.007 = 16.12 \text{ kw/ft}$$

The maximum linear rod power calculated above includes the following allowances:

(1) Calorimetric error - 2%

(2) Stack height shortening - 2%

(3) Effect of local pellet density variations on average fuel temperature at the hot spot (as discussed in Section 4.4) -0.7%

The loss of coolant accident becomes less restrictive with burnup due to clad creepdown. Since the maximum rod power at full rated power is less than the BOL LOCA limit, loss of coolant considerations do not restrict plant power capability.

5.5 CONCLUSIONS

Plant power capability is limited by LOCA, overpower, and DNB safety limits. Restrictions imposed by these limits have been determined with allowance for the effects of fuel densification. The results of these analyses show that the plant can be operated at full rated power without exceeding the limits imposed by a conservative consideration of the effects of fuel densification on plant operation.

FIGURE 5.1

INDIAN POINT UNIT 2
REGION 1
MINIMUM BURNUP ROD WITH DENSIFICATION
FUEL AVERAGE TEMPERATURE
VS
ROD POWER AT VARIOUS OPERATING TIMES

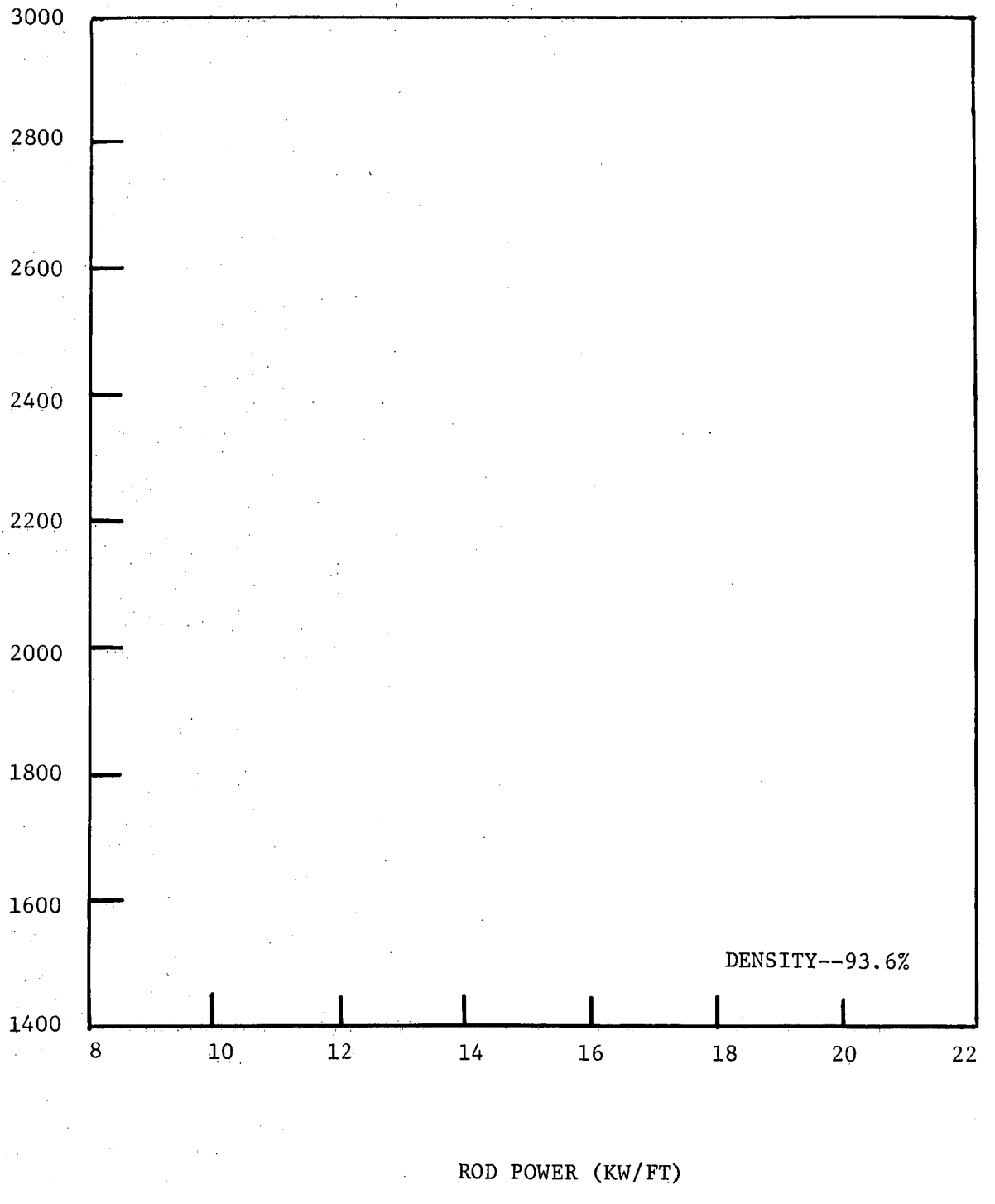

6.0 EFFECTS OF FUEL DENSIFICATION ON ACCIDENT ANALYSIS

6.1 GENERAL

The effects of fuel densification on the design basis and postulated incidents analyzed in the FSAR have been examined. For most cases the effects due to fuel densification can be accommodated within the conservatism used in the FSAR analysis or in the large margins to design basis limits demonstrated by the results presented in the FSAR. Those incidents which are most inclined to impose limitations on plant power capability have been discussed in Section 5.

Calculations have been performed to determine reactivity parameters based on the present core loading. The range of the doppler coefficient (-1.1×10^{-5} to -1.8×10^{-5} $\delta k/k/°F$) is the same as the range for the original design as presented in Table 1.4.1 of the FSAR. The moderator temperature coefficient has a range of $-.35 \times 10^{-4}$ to -3.25×10^{-4} $\delta k/k/°F$ which falls outside the range presented in Table 1.4.1 of the FSAR; however, the range assumed in the accident analysis is 0 to -3.5×10^{-4} $\delta k/k/°F$. Although the boron concentrations given in Table 3.2.1-1 are 50 ppm higher than the values given in Table 1.4.1 of the FSAR, they are well within the conservative values assumed for the Chemical Volume and Control System Malfunction analysis presented in the FSAR. Therefore, the analyses previously presented are valid and conservative with respect to the reactor kinetics characteristics of the present fuel.

6.2 OVERPOWER - OVERTEMPERATURE TRANSIENTS

As discussed in Section 5, anticipated overpower and overtemperature transients will be terminated by the protection system before a DNB ratio of less than 1.30, local linear power density of 21.1 kw/ft or fuel centerline melting temperature is reached. Transients of this type analyzed in the FSAR include:

1) Uncontrolled Control Rod Assembly Withdrawal at Power
2) Excessive Load Increase Incident
3) Excessive Heat Removal Due to Feedwater System Malfunctions

Therefore, the consequences of these accidents are not changed from those noted in the FSAR.

6.3 INCIDENTS WHICH DO NOT REQUIRE REANALYSIS

Uncontrolled Control Rod Assembly Withdrawal from a Subcritical Condition and Startup of an Inactive Loop are non-limiting transients as demonstrated in the FSAR. For these transients, core power and fuel temperatures are much less than the transient overpower limits discussed in Section 5 (i.e., peak heat flux of 45% of nominal for the RCCA Withdrawal incident and maximum nuclear power of 104% of nominal for Inactive Loop Startup, compared to the maximum transient overpower limit of 131.8%). Therefore, fuel densification effects on these transients will not require the imposition of further protection requirements and the consequences of these transients are unchanged from those stated in the FSAR.

Because of the radial pellet shrinkage, there is a resultant increase in core stored energy, which would tend to make the Loss of Normal Feedwater and Loss of AC Power accidents more severe. However, the amount of core stored energy, including densification penalties, has been recalculated, assuming BOL fuel temperatures, and found to be less than 75% of the conservative value assumed in the original FSAR analyses. This, along with the fact that fuel temperature will decrease with burnup, assures that the FSAR analyses as presented are sufficiently conservative and the conclusions are valid as presented.

The Loss of External Load accident presented in the FSAR demonstrated a large margin to DNB. The increase in core stored energy due to densification is considerably less than that for the case assuming a reduction of calculated overall fuel heat transfer coefficient (UA) at beginning of life by a factor of 2 (minimum DNBR, 1.6). The heat flux peaking effects of densification on the DNB ratio are offset by the reduction in design peaking factor, thus the results and conclusions of the previous analysis remain valid.

The Control Rod Assembly Drop incident analyzed in the FSAR demonstrated a large margin to a DNB ratio of 1.30, in terms of core radial peaking factor increase. While densification effects may reduce the allowed

radial peaking factor, the effect on allowed change in the peaking factor will be offset by the reduction in design peaking factor as evidenced by the recalculated core DNB limit curves discussed in Section 5. Action of the rod drop detection circuit in reducing power will further increase margin to DNB and assures that the conclusions about the consequences of this incident as presented in the FSAR are valid.

As discussed in Section 6.1, the reactivity parameters of the revised core loading are within values allowed by the analysis for the various core loading; these parameters are not affected by fuel densification. Thus, the conclusions reached in the FSAR about the CVCS Malfunction accident and the small (credible) steam line breaks are still valid.

For the large (incredible) steamline breaks, the minimum DNB ratio for every case analyzed in the FSAR was greater than 2.0. Physics calculations for the modified core with allowance for fuel densification demonstrated larger shutdown margins and smaller peaking factors than the values assumed in the FSAR analysis. Therefore, the conclusions reached in the FSAR remain valid.

For the Fuel Handling Accident, an evaluation of the effects of fuel densification on the fission product release from the fuel to the gap indicates that the amounts of activity noted in the FSAR are sufficiently conservative to adequately describe any small effects due to relatively small changes in fuel temperature with some compensating effects due to the densification. Thus, the consequences of this accident are not changed from those noted in the FSAR and the Environmental Report.

The Technical Specifications establish the maximum coolant activity based upon limiting the off-site consequences of the assumed steam generator tube rupture. The coolant activity is not affected by fuel densification. Thus, the FSAR and Environmental Report analyses are still valid. Additionally, the results of analyses presented for accidental releases of recycle or waste liquid, waste gas, or a Volume Control Tank accident are also still valid.

6.4 LOSS OF COOLANT ACCIDENT

The effects of fuel densification on the limiting Loss of Coolant Accident have been discussed in Section 5 where it has been determined that the design basis criteria are met for operation at rated power.

The worst case of the spectrum of small break LOCA's has been reanalyzed at rated power to account for fuel densification effects. For this case, the clad temperature increase above the analyses previously submitted is about 60°F, still resulting in peak cladding temperatures well below the limiting value of 2300°F.

Additionally, the effect of increased core stored energy due to fuel densification on the containment energy release transient for the Containment Transient Analysis is more than adequately compensated for by the conservatism included in the FSAR analysis.

6.5 RUPTURE OF CONTROL DRIVE MECHANISM HOUSING, CONTROL ROD EJECTION

6.5.1 INTRODUCTION

The rod ejection transient analysis is performed in two stages; a nuclear power transient calculation and a hot spot fuel heat transfer analysis. As a result of fuel densification, only the hot spot calculation is affected significantly. The effects are:

a) The pellet shrinkage in the radial direction causes the gap heat transfer coefficient to decrease, resulting in an increase in the steady state fuel pellet temperature and therefore the stored energy for a given kw/ft.

b) The axial gap formation causes a local increase in the heat generation rate in an adjacent fuel rod, which may be represented by an increase in the steady-state and transient axial hot channel factor (F_Q^N). This effect increases the fuel stored energy before rod ejection (for at-power cases) and acts as a multiplier on the energy release at the hot spot due to the nuclear transient.

6.5.2 METHOD OF ANALYSIS

Both the nuclear power transient and hot spot heat transfer calculations were repeated for this plant. This was warranted by the core modifications discussed in Chapter 3. The ejected rod worths and hot channel factors were calculated taking into consideration the insertion limits for each case. The insertion limits, assumed for this analysis, are as shown in the Technical Specifications for this plant.

The nuclear power transient was calculated at beginning of life, and end of life, full and zero power. The calculation included a conservative spatial weighting factor as described in Reference 1 applied only to the Doppler feedback, and a conservative choice of trip reactivity including the effect of a stuck rod adjacent to the ejected rod.

The hot spot fuel heat transfer calculation was made for this core using the FACTRAN[2] code. The increase in initial stored energy was taken into account by adjusting the code to give the same steady-state fuel temperature as predicted by a detailed design calculation for the case of densified fuel. The hot spot was assumed to occur in the region of greatest densification, which is the region with the highest fuel temperature for a given kw/ft.

The nuclear power-peaking effect was taken into account by multiplying the steady-state and transient hot channel factors (F_Q) times a peaking factor determined by a statistical study of the effect of distributed axial gaps. A factor to account for pellet stack height reduction was applied to the core average heat flux. For the full power cases a conservative initial hot channel factor F_Q of 2.75 including the densification factor was used.

Departure from nucleate boiling was assumed to occur early in the transient, and the Bishop-Sandberg-Tong correlation[3] was used to obtain the film boiling coefficient. The exothermic Zirconium-steam reaction was taken into account using the Baker-Just parabolic rate equation[4].

The basis for the calculations described above is given in WCAP-7588,[1] and is consistent with the analysis presented in the FSAR. Table 6.1 summarizes the parameters used in the analysis.

6.5.3 RESULTS

The results for the beginning of life and end of life cases are presented below. The effect of part length rods was considered in the analysis of each case.

Beginning of Life, Full Power

Bank D was conservatively assumed to be fully inserted. The worst ejected rod worth and hot channel factor was 0.27% Δk and 5.71, respectively. The

peak hot spot clad average temperature was 2245°F. The peak hot spot fuel center temperature reached 4995°F.

Beginning of Life, Zero Power

For this configuration, banks D+C were assumed fully inserted. The worst ejected rod worth and hot channel factor was 0.74% Δk and 15.3 respectively. The peak hot spot clad average temperature reached only 1285°F, while the fuel center temperature reached 1920°F.

End of Life, Full Power

Again bank D was assumed fully inserted. The ejected rod worth was 0.23% Δk, and the hot channel factor was 4.84. The hot spot transient analysis gave a peak clad average temperature of 1645°F and a pellet center temperature of 4025°F.

End of Life, Zero Power

Again banks C and D were assumed fully inserted. The resulting ejected rod reactivity and hot channel factor was 0.67% Δk and 14.9 respectively. The peak clad average temperature reached 1575°F, and the peak fuel center temperature was 2380°F.

A summary of the cases presented above is given in Table 6.1. The nuclear power and hot spot fuel and clad temperature transients for BOL, HFP case are presented in Figures 6.1 and 6.2.

6.5.4 SUMMARY AND CONCLUSIONS

The cases calculated were beginning of life and end of life, full and zero power. The worst case proved to be the hot full power case at beginning of life. However, this case did not violate the limiting criteria presented in WCAP-7588.[1]

The results of this analysis show that the fuel and clad damage limits presented in WCAP-7588[1] are not exceeded. Therefore, there is no danger of sudden fuel dispersal into the coolant and no danger of consequential damage to the primary coolant loop. Fission product release (if any) will be within the guidelines of 10CFR100.

6.6 LOSS OF REACTOR COOLANT FLOW

6.6.1 LOSS OF FLOW ACCIDENTS

6.6.1.1 General

As demonstrated in the FSAR the most severe credible loss of coolant flow condition occurs upon simultaneous loss of electrical power to all reactor coolant pumps. This incident has been reanalyzed considering the effects of fuel densification on the minimum DNB ratio during the transient. These effects are as follows:

1) Increase in linear heat flux due to fuel stack height reduction.

2) Power spikes due to axial gaps between fuel pellets.

3) Increase in fuel temperatures (and stored energy) due to radial densification and thus, larger pellet clad gap.

Items 1 and 2 cause an increase in the local rod heat flux resulting in a decrease in the minimum core DNB ratio during steady state operation prior to initiation of the transient. Item 3 causes a slower decrease in rod heat flux following reactor trip, resulting in a larger change in DNB ratio during the transient.

6.6.1.2 Analysis and Results

The four pump loss of flow transient was reanalyzed using methods and assumptions consistent with those used in the FSAR with the following exceptions:

1) The core flow coastdown was altered to reflect a conservative representation of the results obtained in plant flow tests. The flow transient assumed is shown in Figure 6.3.

2) The FACTRAN[2] code was used to determine the rod heat flux decay for a range of initial linear rod powers (kw/ft) to determine the value which gives the slowest heat flux decay. This heat flux profile was normalized and applied to the core hot spot for calculation of the DNB ratio. This method is conservative since hot spot heat flux will decrease more rapidly following reactor trip resulting in a higher minimum DNB ratio.

3) Calculations of DNB ratios were made using the steady state THINC code at various time points during the transient using the instantaneous values of core inlet flow and rod heat flux as inputs. This approach is conservative with respect to minimum DNB ratio since it overpredicts fluid enthalpy, at any point in the core, as compared to a transient calculation.

   This results in the calculation of lower minimum DNB ratios than would be predicted by a transient calculation.

4) Calculations of DNB ratios during the transient were made using design basis peaking factors and methodology consistent with that discussed in Section 4.0.

The results of this analysis are shown in Figure 6.3 and Figure 6.4. As can be seen in Figure 6.4 the minimum DNB ratio during the transient does not fall below the limiting value of 1.30.

6.6.1.3 Conclusions

The analysis shows that for the most severe loss of flow transient, i.e., the four pump coastdown, the minimum core DNB ratio does not fall below the limiting value of 1.30. The other cases analyzed in the FSAR demonstrated larger margins to the limiting DNB ratio than the four pump incident (i.e., the FSAR analyses showed minimum DNBR of 1.52 for a 1/4 loss of flow vs. 1.42 for the 4/4 case; all other cases showed greater margins).

Thus we can conclude that all cases would remain above the 1.30 limit and that the conclusions as presented in the FSAR for this incident are still valid.

6.6.2 LOCKED ROTOR

6.6.2.1 General

The hypothetical locked rotor incident was evaluated in the FSAR to determine:

1) Extent of core damage, if any, due to this incident, i.e., number of fuel rods experiencing DNB and peak cladding temperature at the core hot spot.

2) Peak reactor coolant system pressure during the incident.

The effects of fuel densification on those criteria are discussed below:

Coolant System Pressure - The coolant system pressure transient is dependent primarily on core power level prior to the transient and core coolant flow reduction. Fuel densification has a minor effect on this portion of the transient response and the conclusions presented in the FSAR still hold.

Number of Rods Experiencing DNB - Fuel densification effects which contribute to an increase in the number of rods experiencing DNB during the transient are as follows:

1) Increase in fuel pellet temperature and stored energy due to radial densification and thus larger pellet-cladding gap. This effect causes a slower decrease in rod heat flux following reactor trip resulting in a smaller DNB ratio during the transient.

2) Increase in linear flux due to fuel stack height reduction. This effect increases the average rod heat flux by the percentage reduction in stack height.

3) Increase in linear flux due to power spikes caused by axial gaps between fuel rods.

Items 2 and 3 tend to decrease the minimum core DNB ratio in steady state operation prior to the transient.

Peak Cladding Temperature - The effects described above will also serve to cause an increase in peak cladding temperature during the transient. This is due to both the increased stored energy and higher local power peaking.

6.6.2.2 Analysis and Results

The four loop operation locked rotor case was analyzed assuming initial operation at 102% of rated power at BOL. The method of calculating the transient DNB ratio used the assumptions stated in the FSAR with exceptions as noted in the loss of flow analysis of the previous section. Core coolant flow was determined assuming an instantaneous seizure of a reactor coolant pump rotor with data based upon the results of the plant flow tests.

The resulting core flow transient is shown in Figure 6.5. The minimum DNB ratio was calculated to be 1.375 as shown in Figure 6.6. A clad temperature calculation was not performed since the minimum DNB ratio at the hot spot did not go below 1.30, thus DNB would not be expected to occur during the transient.

6.6.2.3 Conclusions

The benefits obtained from a reduction in the design peaking factors have more than compensated for the detrimental effects of fuel densification on the locked rotor transient. Since DNB does not occur during the transient, there will be no damage to the fuel or cladding, and hence no fission product release to the reactor coolant.

References for Section 6

1) D. H. Risher, Jr., "An Evaluation of the Rod Ejection Accident in Westinghouse Pressurized Water Reactors Using Spatial Kinetics Method," WCAP-7588, Rev. 1, December, 1971.

2) H. G. Hargrove, "FACTRAN - A FORTRAN IV Code for Thermal Transients in a UO_2 Fuel Rod," WCAP-7908, July, 1972.

3) A. A. Bishop, R. O. Sandberg, L. S. Tong, "Forced Convection Heat Transfer at High Pressure After the Critical Heat Flux," ASME 65-HT-31, 1965.

4) L. Baker, Jr. and J. C. Just, "Studies of Metal Water Reactions at High Temperature," ANL-6548, 1962.

TABLE 6.1

SUMMARY OF ROD EJECTION ANALYSIS PARAMETERS

Time in Life		Beginning	Beginning	End	End
Power Level		102%	0%	102%	0%
Ejected rod worth %Δk		.27	.74	.23	.67
Delayed neutron fraction %Δk		0.7	0.7	0.5	0.5
Feedback reactivity weighting		1.2	2.2	1.2	1.9
Trip rod shutdown %Δk		5.0	3.0	4.0	1.5
Prompt neutron lifetime	Microseconds	18	18	16	16
F_Q before rod ejection		2.75	--	2.75	--
F_Q after rod ejection		5.71	15.3	4.84	14.9
Number of operating pumps		4	2	4	2
Max, fuel pellet average temperature	°F	3840	1650	2905	2065
Max, fuel center temperature	°F	4995	1920	4025	2380
Max. clad temperature	°F	2245	1285	1645	1575

Figure 6.1

Nuclear Power Transient
BOL HFP

Rod Ejection Accident

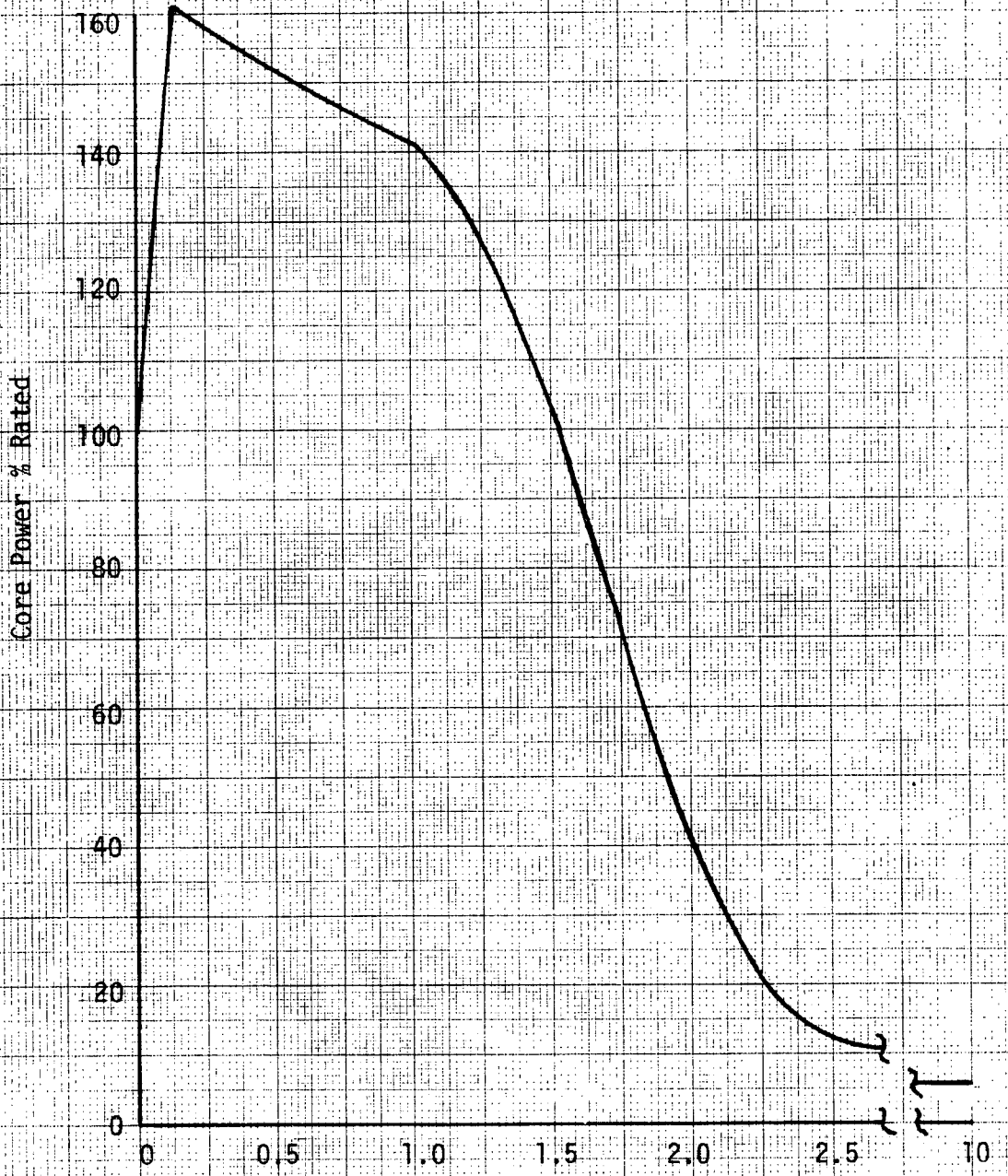

Figure 6.2

Hot Spot Fuel and Clad
Temperature vs Time, BOL HFP

Rod Ejection Accident

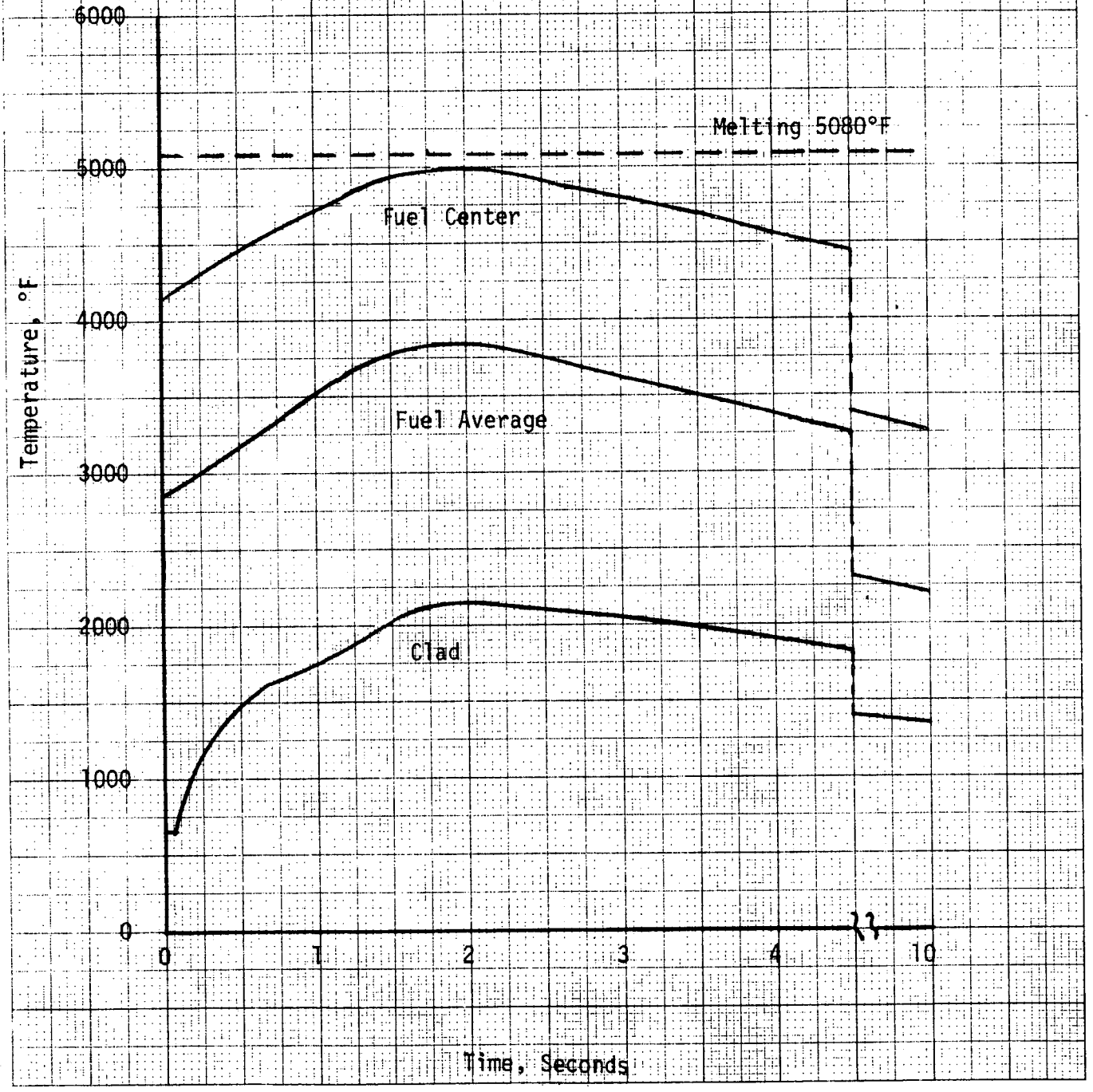

FIGURE 6.3

LOSS OF FLOW ANALYSIS

4/4 PUMPS COASTING DOWN

CORE FLOW VS. TIME

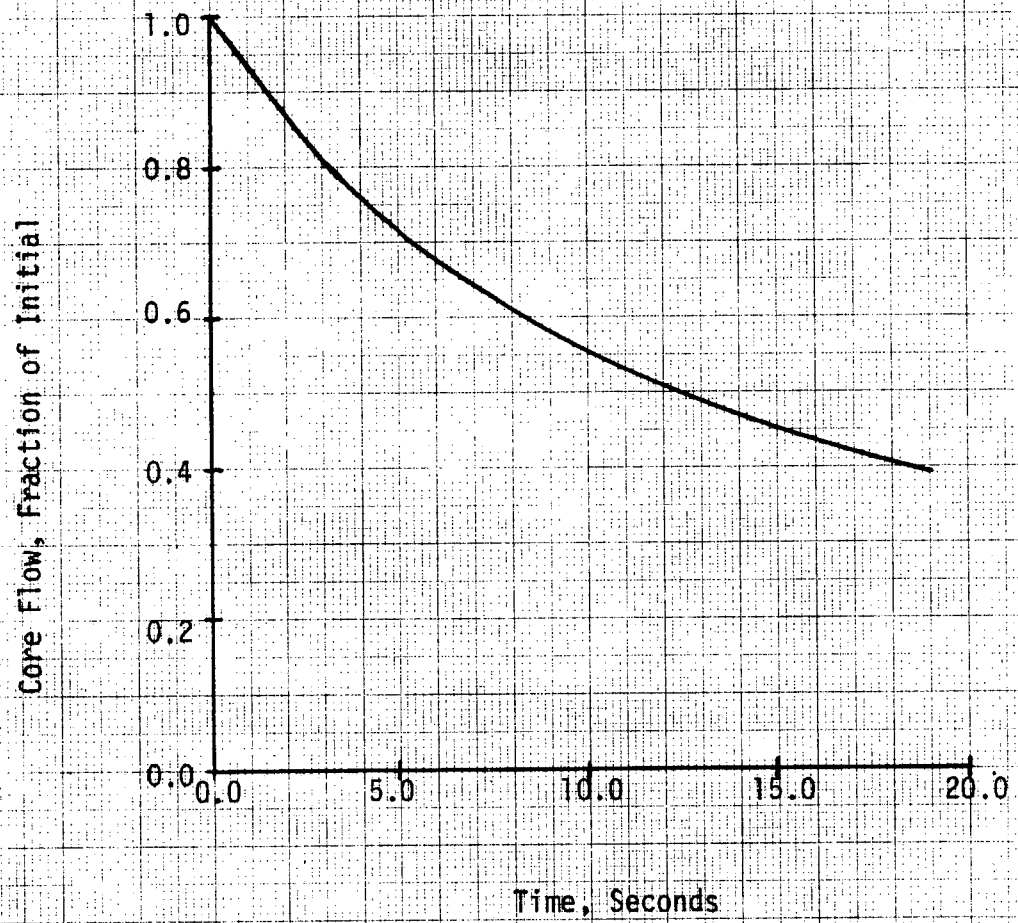

FIGURE 6.4

LOSS OF FLOW ANALYSIS

4/4 PUMPS COASTING DOWN

DNB RATIO VS. TIME

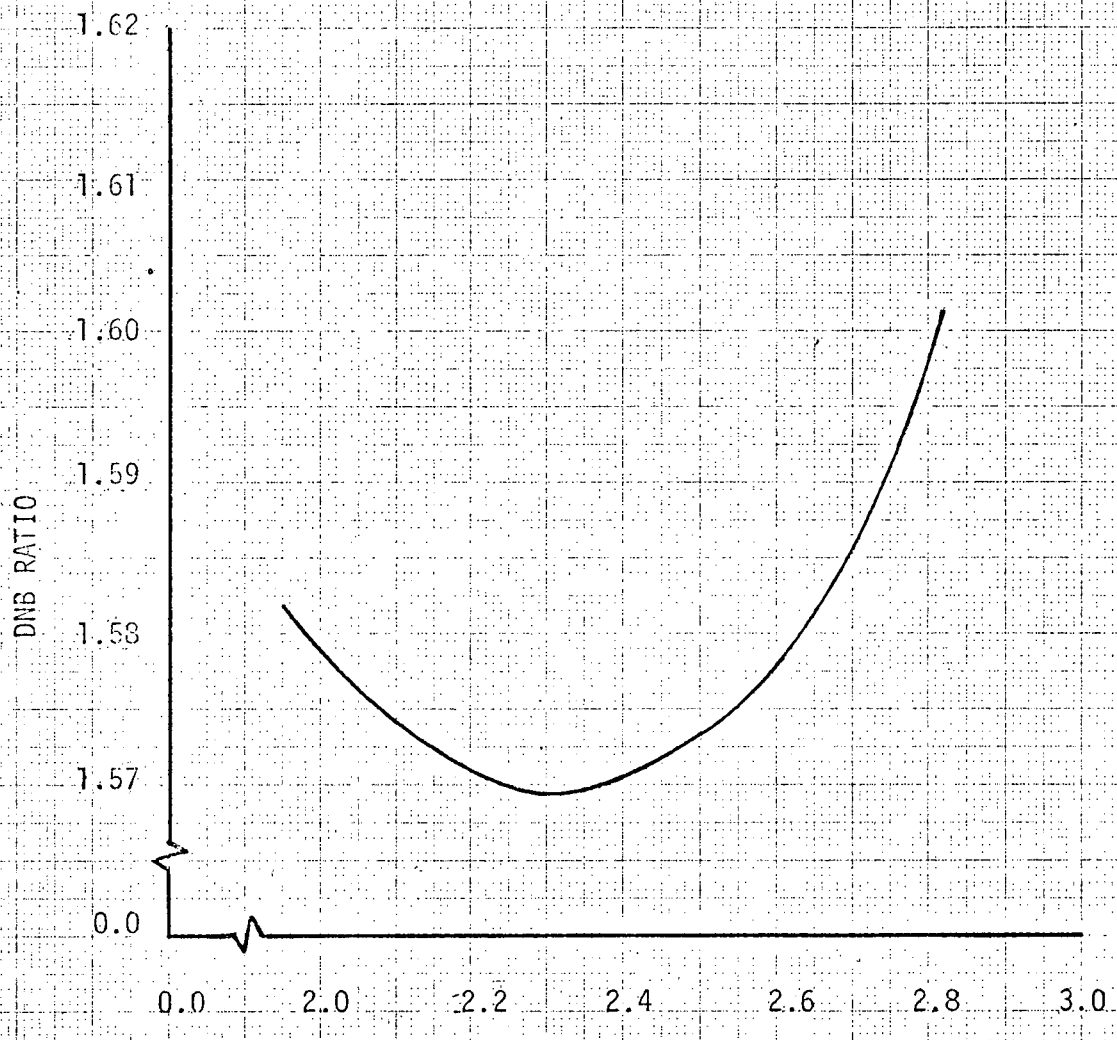

FIGURE 6.5

LOCKED ROTOR ANALYSIS

CORE FLOW VS. TIME

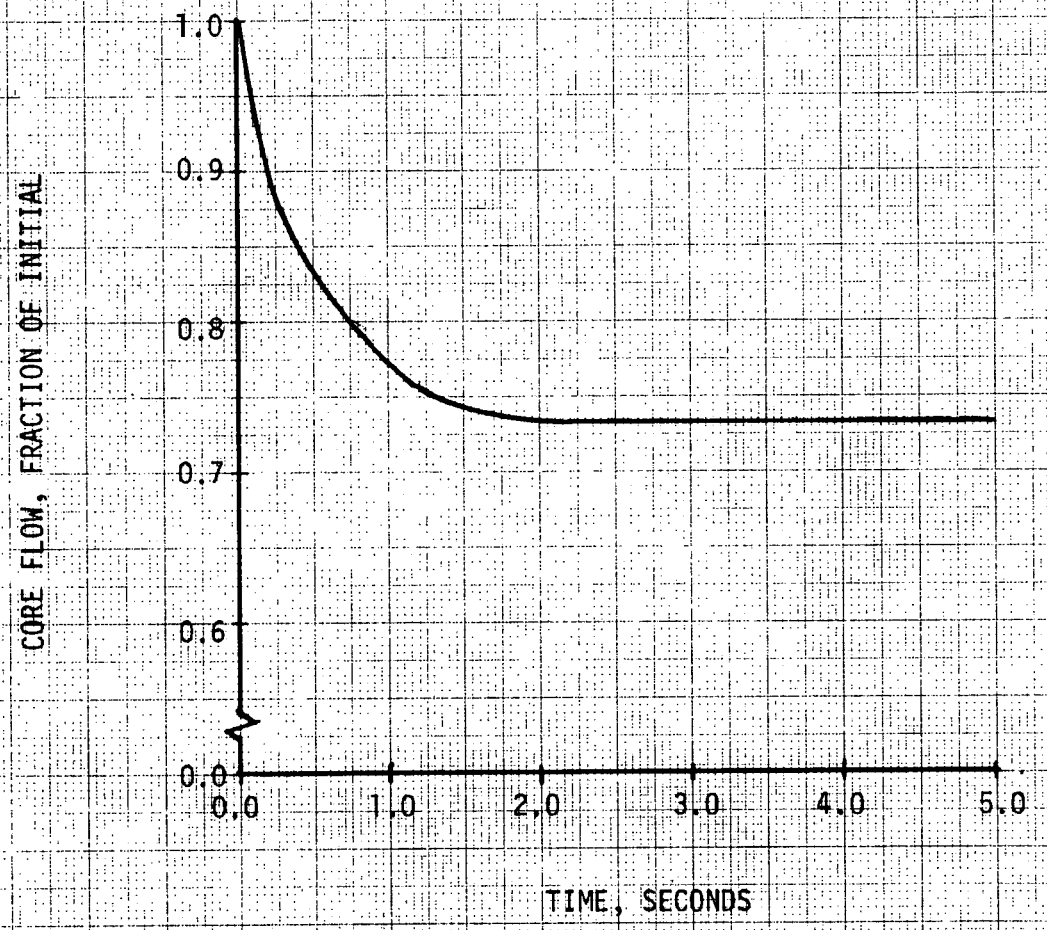

FIGURE 6.6

LOCKED ROTOR ANALYSIS

MINIMUM DNB RATIO VS. TIME

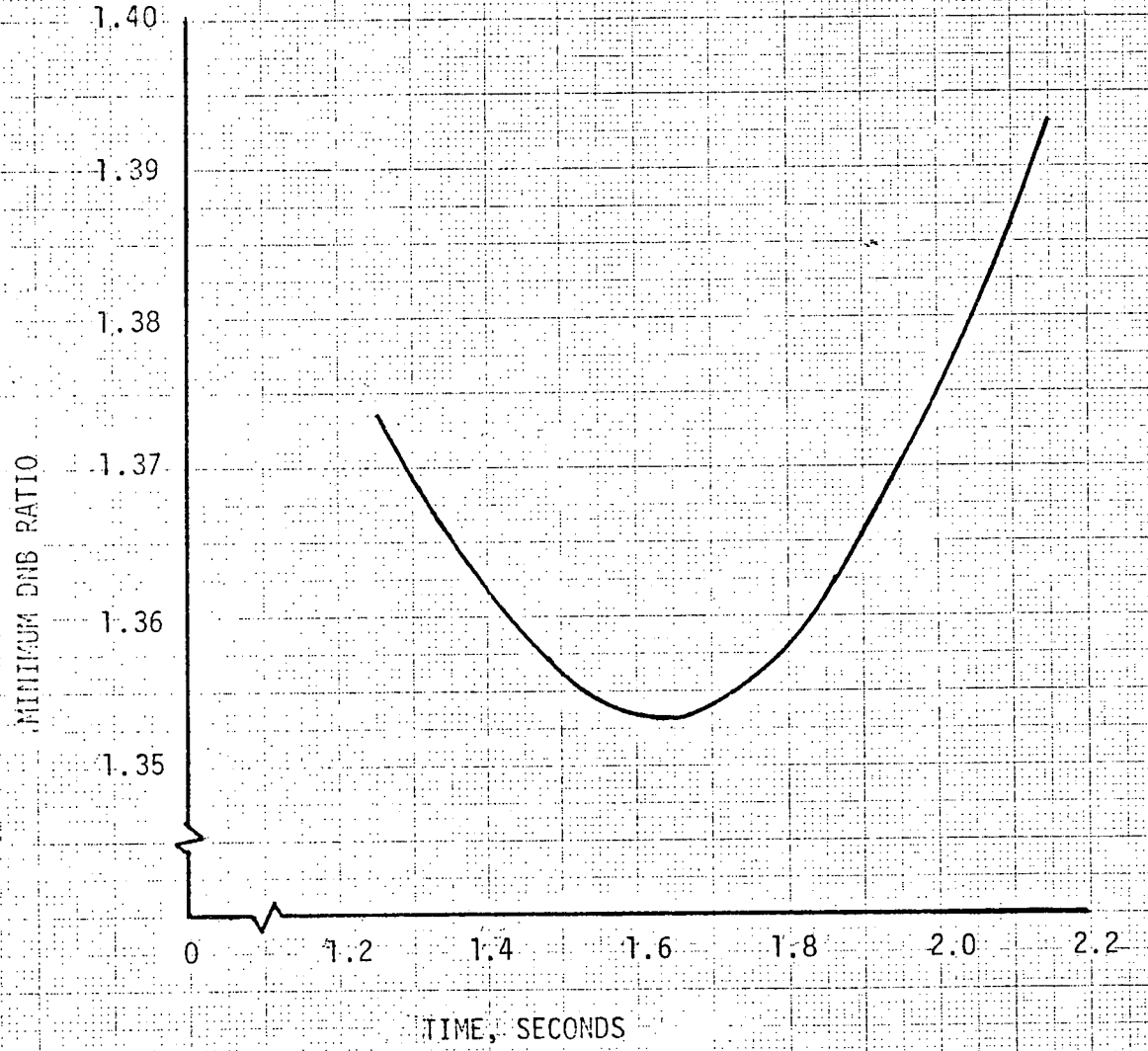

7.0 REVISIONS TO TECHNICAL SPECIFICATIONS

In order to allow for the effects of fuel densification during plant operation, the following revisions shall apply to the Technical Specifications as previously submitted. All specifications not explicitly revised shall remain as stated in the original submittal. The paragraph numbering of the original Technical Specifications are retained for convenience of referencing.

Section 2.3 LIMITING SAFETY SETTINGS, PROTECTIVE INSTRUMENTATION

Specification:

Protective instrumentation for reactor trip settings shall be as follows (referenced part of specification noted in parenthesis);

[1.B. (5)] Overpower ΔT

$$\leq \Delta T_o \left[K_4 - K_5 \frac{dT}{dt} - K_6 (T - T') - f(\Delta I)\right]$$

where

ΔT_o = Indicated ΔT at rated power
T = Average temperature, °F
T' = Indicated T_{avg} at nominal condition at rated power, 570°F
$K_4 \leq 1.19$
K_5 = Zero for decreasing average temperature
$K_5 \geq 0.188$, for increasing average temperature (sec/°F)
$K_6 \geq 0.0019$ for $T \geq T'$; $K_6 = 0$ for $T < T'$
$\frac{dT}{dt}$ = Rate of change of T_{avg}

and $f(\Delta I)$ is a function of the indicated difference between top and bottom detectors of the power-range nuclear ion chambers; with gains to be selected based on measured instrument response during plant startup tests such that:

1. For $(q_t - q_b)$ within the range between ΔI_1 and ΔI_2 given in the table below, $f(\Delta I) = 0$ (where q_t and q_b are percent power in the top and bottom halves of the core respectively, and $q_t + q_b$ is total core power in percent of rated power)

2. For each percent that $(q_t - q_b)$ is less than ΔI_1 or greater than ΔI_2, the Delta-T trip set point shall be automatically reduced by 2% of its value at rated power.

ΔI_1 and ΔI_2 are linear functions of the gain K_4. The proper limits on ΔI_1 and ΔI_2 shall be obtained from the following table which gives the allowable values corresponding to the actual value of K_4.

K_4	ΔI_1	ΔI_2
$\leq$ 1.01	$\geq$ -21	$\leq$ +16
1.04	$\geq$ -19.5	$\leq$ +14.5
1.07	$\geq$ -18	$\leq$ +13
1.10	$\geq$ -16.5	$\leq$ +11.5
1.13	$\geq$ -15	$\leq$ +10
1.16	$\geq$ -13.5	$\leq$ +8.5
1.19	$\geq$ -12	$\leq$ +7

Basis for Revision:

The f(ΔI) function in overpower and overtemperature protection system setpoints have been revised to include effects of fuel densification on core safety limits. Thy revised setpoints as given above will ensure that the safety limit of centerline fuel melt will not be reached and DNBR of 1.30 will not be violated.

Section 3.10 CONTROL ROD AND POWER DISTRIBUTION LIMITS

Specification:

The referenced portion of the previous specification is noted in parenthesis.

(3.10.1) Control Rod Insertion Limits

(3.10.1.5) The part length rods shall not be more than 70% inserted.

(3.10.2) Power Distribution Limits and Misaligned Control Rod

(3.10.2.1) (Change 50% to 75%)

(3.10.2.2-b) The hot channel factors shall be determined and maximum allowable power shall be reduced one percent for each percent the hot channel factors exceed the design values of:

$$F_Q^N \leq 2.62\ [1 + 0.2(1-P)]$$ in the indicated flux difference range of +7 to -12 percent

$$F_{\Delta H}^N \leq 1.65\ [1 + 0.2(1-P)]$$

where P is the fraction of full power at which the core is operating.

For every percent outside of the indicated flux difference range +7 to -12 percent, the allowed F_Q^N may be increased above 2.62 by two percent.

The measured values, with due allowance for measurement error, must be corrected by including a penalty as shown on Figure 3.10-4 (at the approximate core location) to account for fuel densification effects before comparison with the limiting values above.

(3.10.2.6) Except during physics tests, the following power distribution restrictions must be maintained:

a. At rated power, the indicated axial flux difference must be maintained within +7 percent and -12 percent.

b. If, at rated power, the indicated axial flux difference exceeds the permissible range defined above for a period of more than eight hours, the situation shall be corrected or the reactor power shall be reduced 2 percent, for each percent the flux difference exceeds the permissible range.

c. For every 2 percent below full power, the permissible flux difference range is extended by 1 percent.

Basis for Revision:

Part length rod insertion has been limited to eliminate certain adverse power shapes.

Two criteria have been chosen as a design basis for fuel performance related to fission gas release, pellet temperature and cladding mechanical properties. First, the peak value of linear power density must not exceed 21.1 kw/ft. Second, the minimum DNBR in the core must not be less than 1.30 in normal operation or in short term transients.

In addition to the above, the initial steady state conditions for the peak linear power for a loss of coolant accident must not exceed the values assumed in the accident evaluation. This limit is required in order for the maximum clad temperature to remain below that established by the Interim Policy Statement for LOCA. To aid in specifying the limits on power distribution the following hot channel factors are defined.

F_Q, Heat Flux Hot Channel Factor, is defined as the maximum local heat flux on the surface of a fuel rod divided by the average fuel rod heat flux, allowing for manufacturing tolerances on fuel pellets and rods.

F_Q^N, Nuclear Heat Flux Hot Channel Factor is defined as the maximum local fuel rod linear power density divided by the average fuel rod linear power density, assuming nominal fuel pellet and rod dimensions.

F_Q^E, Engineering Heat Flux Hot Channel Factor is defined as the ratio between F_Q, and F_Q^N and is the allowance on heat flux required for manufacturing tolerances.

$F_{\Delta H}^N$, nuclear Enghalpy Rise Hot Channel Factor, is defined as the ratio of the integral of linear power along the rod on which minimum DNBR occurs to the average rod power.

It should be noted that $F_{\Delta H}^N$ is based on an integral and is used as such in the DNB calculations. Local heat fluxes are obtained by using hot channel and adjacent channel explicit power shapes which take into account variations in horizontal (x-y) power shapes throughout the core. Thus the horizontal power shape at the point of maximum heat flux is not necessarily directly related to $F_{\Delta H}^N$.

It has been determined by analysis that the design limits on peak local power density on minimum DNBR at full power and LOCA are met, provided:

$$F_Q^N \leq 2.62 \text{ and } F_{\Delta H}^N \leq 1.65$$

These qualities are measurable although there is not normally a requirement to do so. Instead it has been determined that, provided certain conditions are observed, the above hot channel factor limits will be met; these full power conditions are as follows.

1. Control rods in a single bank move together with no individual rod insertion differing by more than 15 inches from the bank demand position.

2. Control rod banks are sequenced with overlapping banks as described in Technical Specification 3.10-1.

3. The control bank insertion limits are not violated.

4. Axial power distribution guide lines, which are given in terms of flux difference control, are observed. Flux difference refers to the difference in signals between the top and bottom halves of two-section excore neutron detectors. The flux difference is a measure of the axial offset which is defined as the difference in power between the top and bottom halves of the core. Calculation of core average axial peaking factors have been correlated with axial offset. The correlation shows that an F_Q^N of 2.62 and allowed DNB shapes, including the effects of fuel densification, are not exceeded if the axial offset (flux difference) is maintained between -15 and +10 percent.

For operation at the fraction, P, of full power the design limits are met, provided,

$$F_Q^N \leq 2.62\ [1 + 0.2\ (1-P)]$$ in the indicated flux difference range range of +7 to -12 percent.

and

$$F_{\Delta H}^N \leq 1.65\ [1 + .2\ (1-P)]$$

For every percent outside of the indicated flux difference range +7 to -12 percent, the allowed F_Q^N may be increased above 2.62 by two percent.

The permitted relaxation of F_Q^N and $F_{\Delta H}^N$ allows radial power shape changes with rod insertion to the insertion limits. The allowed increase in F_Q^N for large flux differences is consistent with power shapes assumed in setting the overpower and overtemperature ΔT setpoints. It has been determined that provided the above conditions 1 through 4 are observed, these hot channel factors limits are met.

For normal operation and anticipated transients the core is protected from exceeding 21.1 KW/ft locally, and from going below a minimum DNBR of 1.30, by automatic protection on power, flux difference, pressure and temperature. Only condition 1 through 3, above, are mandatory since the flux difference is an explicit input to the protection system.

Measurements of the hot channel factors are required as part of start-up physics tests and whenever abnormal power distribution conditions require a reduction of core power to a level based on measured hot channel factors.

In the specified limit of F_Q^N there is a 5 percent allowance for uncertainties[1] which means that normal operation of the core within the defined conditions and procedures is expected to result in $F_Q^N \leq 2.62/1.05$ even on a worst case basis. When a measurement is taken experimental error must be allowed for and 5 percent is the appropriate allowance for a full core map taken with the moveable incore detector flux mapping system.

In the specified limit of $F_{\Delta H}^N$ there is a 10 percent allowance for uncertainties[1] which means that normal operation of the core is expected to result in $F_{\Delta H}^N \leq 1.65/1.10$. The logic behind the larger uncertainty in this case is that (a) abnormal perturbations in the radial power shape (e.g. rod misalignment) affect $F_{\Delta H}^N$ and (b) the operator has a direct influence on F_Q^N, through movement of part length rods, and can limit it to the desired value, he has no direct control over $F_{\Delta H}^N$ and (c) an error in the predictions for radial power shape, which may be detected during startup physics tests can be compensated for in F_Q^N by tighter axial control, but compensation for $F_{\Delta H}^N$ is less readily available. Five percent is the appropriate allowance for a full core map taken with the movable in-core detector flux mapping system.

Section 5.3 REACTOR

Applicability

Applies to the reactor core, reactor coolant system, and emergency core cooling systems.

Objective

To define those design features which are essential in providing for safe system operations.

A. Reactor Core

1. The reactor core contains approximately 87 metric tons of uranium in the form of slightly enriched uranium dioxide pellets. The pellets are encapsulated in Zircaloy-4 tubing to form fuel rods. The reactor core is made up of 193 fuel assemblies. Each fuel assembly contains 204 fuel rods.(1)

2. The average enrichment of the initial core is a nominal 2.8 weight per cent of U-235. Three fuel enrichments are used in the initial core. The highest enrichment is a nominal 3.3 weight per cent of U-235.(2)

3. Reload fuel will be similar in design to the initial core. The enrichment of reload fuel will be no more than 3.4 weight per cent of U-235.

4. Burnable poison rods are incorporated in the initial core. There are 1412 poison rods in the form of 7,8,9,12,16 and 20-rod clusters, which are located in vacant rod cluster control guide tubes.(3) The burnable poison rods consist of borated pyrex glass clad with stainless steel.(4)

5. There are 53 full-length RCC assemblies and 8 partial-length RCC assemblies in the reactor core. The full-length RCC assemblies contain a 142 inch length of silver-indium-cadmium alloy clad with the stainless steel. The partial-length RCC assemblies contain a 36 inch length of silver-indium-cadmium alloy with the remainder of the stainless steel sheath filled with Al_2O_3. (5)

B. Reactor Coolant System

1. The design of the reactor coolant system complies with the code requirements. (6)

2. All piping, components and supporting structures of the reactor coolant system are designed to Class I requirements, and have been designed to withstand the maximum potential seismic ground acceleration, 0.15g, acting in the horizontal and 0.10g acting in the vertical planes simultaneously with no loss of function.

3. The total liquid volume of the reactor coolant system, at rated operating conditions, is 11,350 cubic feet.

References

(1) FSAR Section 3.2.2 and Section 3 of this report
(2) FSAR Section 3.2.1 and Section 3 of this report
(3) FSAR Section 3.2.1 and Figure 3.3 of this report
(4) FSAR Section 3.2.3
(5) FSAR Sections 3.2.1 & 3.2.3
(6) FSAR Table 4.1-9

Figure 3.10-4

Power Spike Factor vs Elevation

IPP2, Cycle 1